S-CUBED
A Division of Maxwell Laboratories, Inc.

SSS-R-88-9213

FURTHER STUDIES OF SEISMIC VARIABILITY AT THE SHAGAN RIVER TEST SITE

B. W. BARKER
J. R. MURPHY

FINAL REPORT

PREPARED FOR:
U. S. ARMS CONTROL AND DISARMAMENT AGENCY
WASHINGTON, DC 20451

CONTRACT NO. AC5MC112

DECEMBER, 1987

P. O. Box 1620, La Jolla, California 92038-1620
(619) 453-0060

50272-101

REPORT DOCUMENTATION PAGE	1. REPORT NO.	2.	Recipient's Accession No.

4. Title and Subtitle

FURTHER STUDIES OF SEISMIC VARIABILITY AT THE SHAGAN RIVER TEST SITE

5. Report Date
Approved January 1988

6.

7. Author(s)
Brian W. Barker and John R. Murphy

8. Performing Organization Rept. No.
SSS-R-88-9213

9. Performing Organization Name and Address

S-Cubed, A Div. of Maxwell Laboratories, Inc.
P.O. Box 1620
La Jolla, California 92038-1620

10. Project/Task/Work Unit No.

11. Contract(C) or Grant(G) No.
(C) AC5MC112
(G)

12. Sponsoring Organization Name and Address

U.S. Arms Control and Disarmament Agency
Bureau of Verification and Intelligence
320 21st Street, N.W.
Washington, DC 20451

13. Type of Report & Period Covered
FINAL REPORT
SEP 1986 - SEP 1987

14.

15. Supplementary Notes

(m sub b)

16. Abstract (Limit: 200 words)

Large samples of teleseismic P wave data recorded from Shagan River underground explosions have been systematically analyzed in an attempt to develop a better quantitative understanding of the sources of m_b variability observed for these explosions. Results indicate that large differences in station-corrected m_b residuals between explosions in close proximity are associated with changes in the near-source P wave propagation paths to teleseismic distances. Projection of the m_b residuals from seismic stations in continental Europe back into the corresponding P wave initiation area near the source reveals the existence of an anomalous volume of material located northwest of the test site at a depth of about 100 km. This anomalous volume apparently defocuses energy out of paths to certain stations and redirects this energy into the paths to other stations. Presumably this anomalous volume corresponds to some sharp lateral variation in physical properties, in particular P wave velocity, at this depth. Available geologic maps indicate no surface expression of this anomaly.

In some cases, the observed patterns of m_b residual variation can be correlated with similar patterns of variation in either spectral composition, coda complexity or arrival times of the P wave signals. The sense of these variations is such that enhanced high frequency energy, decreased coda complexity and delayed arrival times are all associated with a positive shift in the m_b residuals.

17. Document Analysis a. Descriptors

Explosion Seismology
Threshold Test Ban Treaty

b. Identifiers/Open-Ended Terms

Shagan River
GDSN
Body Waves
m_b
Focusing/Defocusing
Ray Tracing

c. COSATI Field/Group Seismology

18. Availability Statement:

Release Unlimited.

19. Security Class (This Report)	21. No. of Pages
UNCLASSIFIED	80
20. Security Class (This Page)	**22. Price**
UNCLASSIFIED	

(See ANSI-Z39.18) See Instructions on Reverse

OPTIONAL FORM 272 (4-77)
(Formerly NTIS-35)
Department of Commerce

TABLE OF CONTENTS

LIST OF ILLUSTRATIONS

LIST OF ILLUSTRATIONS (Continued)

LIST OF ILLUSTRATIONS (Continued)

I. INTRODUCTION

In 1974, the U.S. and U.S.S.R. signed a Threshold Test Ban Treaty (TTBT) which prohibits the testing of underground nuclear explosions with yields greater than 150 kilotons. Upon ratification, the treaty calls for the bilateral exchange of certain geologic and geophysical data, as well as the yields of two calibration events, in each so-called "geophysically distinct" testing area, in order to facilitate verification of treaty compliance. Although not defined explicitly in the TTBT protocol, the term "geophysically distinct" is intended to denote an area within which the geophysical parameters controlling the magnitude-yield relationship are uniform; that is, an area within which a single yield-scaling relation holds for all explosions. However, a problem arises in that for areas such as the principal U.S.S.R. underground nuclear testing areas near Semipalatinsk, it is not obvious how such geophysically distinct areas can be recognized using information known to us at the present time. For this reason, over the past several years we have been conducting a series of research investigations directed toward assessing the feasibility of using teleseismic P wave data recorded from explosions to identify geophysically distinct testing areas within the Shagan River region of the Semipalatinsk test site.

In a previous study, Dermengian et al. (1985) demonstrated that there are pronounced variations in m_b residuals as a function of explosion location within the Shagan River test site and suggested that these variations may be related to lateral variations in the subsurface geologic structure beneath the test site. This inference was based on analyses of large samples of teleseismic P wave amplitude and arrival time data recorded from explosions at this test site and on detailed comparisons of m_b residual data at common stations from selected pairs of explosions. Thus, the results of that preliminary study indicated that the teleseismic data may indeed be useful for identifying geophysically distinct testing areas within the Shagan River test site. In Barker and Murphy (1986), this investigation was extended to include an analysis of possible effects of tectonic release on the observed short-period P waves. The results of

that study indicated that, although the available evidence was not sufficient to rule out the possibility that tectonic release might be introducing systematic positive bias into the network-averaged m_b values assigned to some Shagan River explosions, it was possible to conclude that the observed short-period teleseismic P wave amplitudes did not show any statistically significant azimuthal variations which could be correlated with a tectonic radiation pattern. That is, the systematic variations of single station m_b residuals with explosion location at Shagan River documented by Dermengian et al. (1985) do not correlate with the levels of tectonic release inferred from the long-period surface wave data. Thus, the analyses conducted to date support the hypothesis that there are near-source, non-axisymmetric geologic structures beneath the Shagan River test area which produce differences in the coupling of seismic energy into the various teleseismic P wave propagation paths.

This report describes the results of a follow-on study conducted with the objectives of improving the resolution of the sources of observed P wave variability at Shagan River and of correlating these inferred sources with available independent geological and geophysical information about the test site. The report consists of four sections including these introductory remarks. In Section II we describe and analyze the P wave amplitude data collected for this project and use the results of this analysis to define regions of apparent subsurface structural variation at Shagan River. We then attempt to interpret these results in terms of specific subsurface structural features beneath the test site. In Section III we describe a preliminary analysis of waveform data from a subset of the explosions aimed at defining the near-source structural contributions to the waveform time- and frequency-domain characteristics. In Section IV we summarize our main results and present our conclusions regarding the nature of teleseismic P wave and P coda variations from Shagan River explosions.

II. m_b DATA ANALYSIS

2.1 REVIEW OF PREVIOUS WORK

The explosion sample analyzed in this report is the same as that described and analyzed in Dermengian et al. (1985). That is, it consists of 52 Shagan River explosions occurring in the time interval 1964 to 1982 which have been assigned m_b values of greater than 5.5 by the ISC. Epicenter locations for these events, as determined by a Joint Epicenter Determination (JED) method (Marshall et al., 1984), are displayed graphically in Figure 1, where it can be seen that they are fairly evenly distributed across the Shagan River testing area. The event numbers shown in Figure 1 refer to Table 1 of this report where detailed origin information for the events can be found.

In Dermengian et al. (1985), a least squares analysis was performed on a large number of single station m_b readings for these explosions, resulting in network-averaged m_b values for the events and average station corrections for a set of 59 worldwide stations used in the analysis. The "station corrections" determined by this method actually represent the composite of effects at the source, along the propagation path and at the receiver which cause the m_b values at a particular station to be consistently different from the corresponding large network average m_b values. Thus, for explosions at a particular test site such as Shagan River, variations of the "station corrections" with source location within the test site would be more closely associated with propagation effects near the source than with variations in the crustal structure beneath the receivers. Using these station corrections and the network-averaged m_b values, station-corrected m_b residuals (i.e., corrected single station m_b - event m_b) were then computed for all event-station pairs and analyzed as a function of station and source location. Dermengian et al. (1985) demonstrated that explosions located in the central and northeast sections of the Shagan River test area show pronounced m_b residual patterns as a function of source-to-station azimuth which vary greatly from explosion to explosion, while patterns from events in the southwest are much more regular. Furthermore, these variations in azimuthal m_b patterns appear to be related to event location rather than tectonic release effects and,

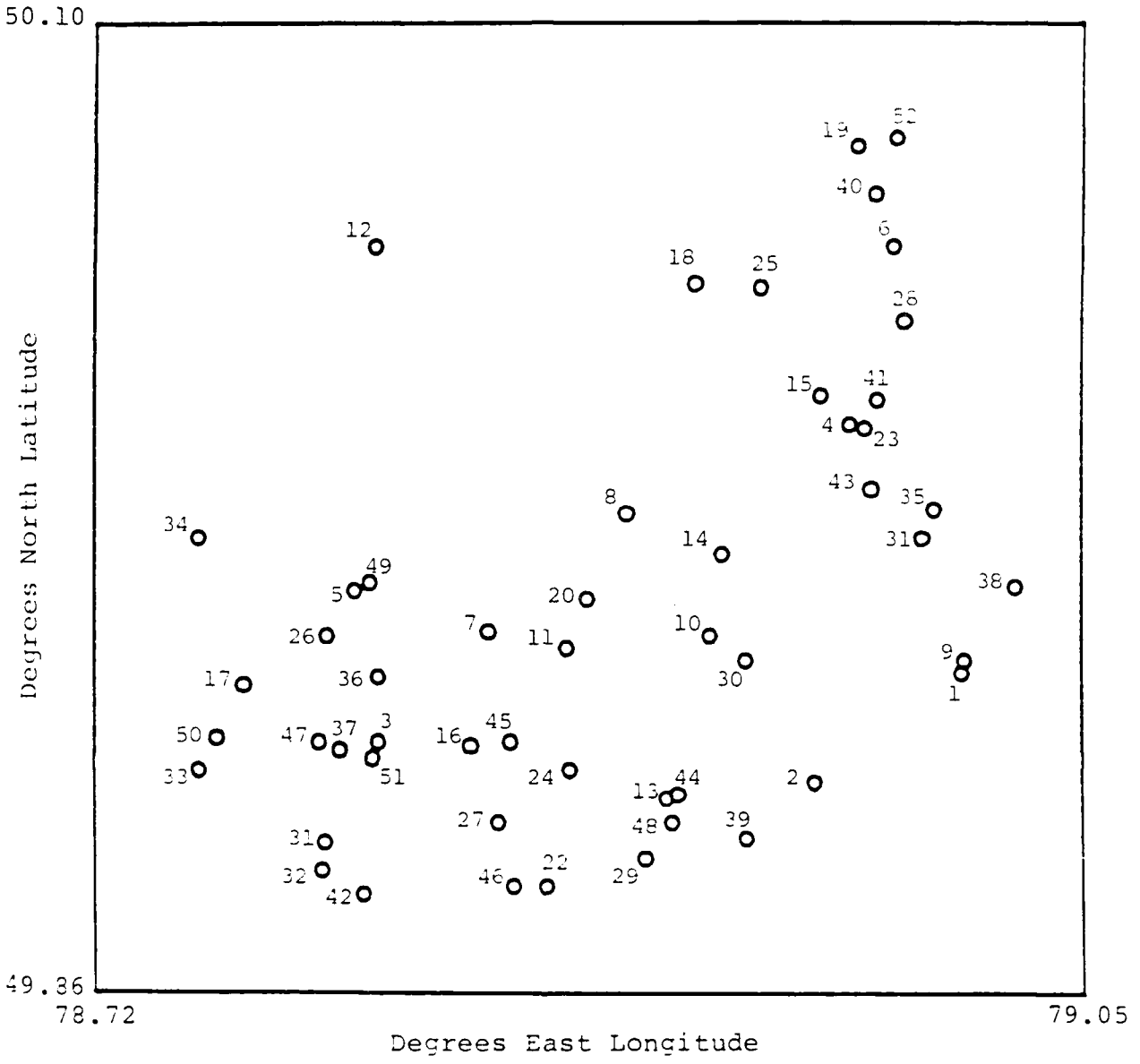

Figure 1. JED locations for the Shagan River explosions of Table 1.

Table 1

SOURCE PARAMETERS FOR SHAGAN RIVER EXPLOSIONS

Event #	Date	Origin Time	Lat.(N)	Long.(E)	m_b
01	01/15/65	05:59:58.4	49.940	79.010	5.94
02	11/30/69	03:32:57.1	49.913	78.961	5.99
03	11/02/72	01:26:57.6	49.923	78.815	6.25
04	12/10/72	04:27:07.3	50.001	78.973	5.93
05	07/23/73	01:22:57.6	49.962	78.812	6.34
06	12/14/73	07:46:57.1	50.044	78.987	5.83
07	05/31/74	03:26:57.5	49.950	78.852	5.86
08	10/16/74	06:32:57.6	49.979	78.898	5.49
09	12/27/74	05:46:56.9	49.943	79.011	5.57
10	04/27/75	05:36:57.2	49.949	78.926	5.59
11	10/29/75	04:46:57.3	49.946	78.878	5.65
12	12/25/75	05:16:57.2	50.044	78.814	5.67
13	07/04/76	02:56:57.5	49.909	78.911	5.85
14	08/28/76	02:56:57.5	49.969	78.930	5.92
15	11/23/76	05:02:57.3	50.008	78.963	5.95
16	12/07/76	04:56:57.4	49.922	78.846	5.92
17	05/29/77	02:56:57.6	49.937	78.770	5.72
18	09/05/77	03:02:57.3	50.035	78.921	5.83
19	10/29/77	03:07:02.5	50.069	78.975	5.54
20	11/30/77	04:06:57.4	49.958	78.885	5.91
21	06/11/78	02:56:57.6	49.898	78.797	5.82
22	07/05/78	02:46:57.5	49.887	78.871	5.82
23	08/29/78	02:37:06.2	50.000	78.978	5.94
24	09/15/78	02:36:57.4	49.916	78.879	5.99
25	11/04/78	05:05:57.3	50.034	78.943	5.57
26	11/29/78	04:33:02.5	49.949	78.798	5.99
27	06/23/79	02:56:57.5	49.903	78.855	6.18
28	07/07/79	03:46:57.3	50.026	78.991	5.82

Table 1 (Continued)

SOURCE PARAMETERS FOR SHAGAN RIVER EXPLOSIONS

Event #	Date	Origin Time	Lat.(N)	Long.(E)	m_b
29	08/04/79	03:56:57.1	49.894	78.904	6.16
30	08/18/79	02:51:57.1	49.943	78.938	6.19
31	10/28/79	03:16:56.9	49.973	78.997	5.97
32	12/02/79	04:36:57.4	49.891	78.786	6.00
33	12/23/79	04:56:57.4	49.916	78.755	6.16
34	04/25/80	03:56:57.5	49.973	78.755	5.45
35	06/12/80	03:26:57.6	49.980	79.001	5.53
36	06/29/80	02.32:57.7	49.939	78.815	5.70
37	09/14/80	02:42:39.1	49.921	78.802	6.22
38	10/12/80	03:34:14.1	49.961	79.028	5.87
39	12/14/80	03:47:06.4	49.899	78.938	5.97
40	12/27/80	04:09:08.1	50.057	78.981	5.87
41	03/29/81	04:03:50.0	50.007	78.982	5.57
42	04/22/81	01:17:11.3	49.885	78.810	5.92
43	05/27/81	03:58:12.3	49.985	78.980	5.30
44	09/13/81	02:17:18.2	49.910	78.915	6.09
45	10/18/81	03:57:02.6	49.923	78.859	6.03
46	11/29/81	03:35:08.6	49.887	78.860	5.61
47	12/27/81	03:43:14.1	49.923	78.795	6.28
48	04/25/82	03:23:05.4	49.903	78.913	6.11
49	07/04/82	01:17:14.2	49.960	78.807	6.22
50	08/31/82	01:31:00.7	49.924	78.761	5.36
51	12/05/82	03:37:12.5	49.919	78.813	6.18
52	12/26/82	03:35:14.2	50.071	78.988	5.72

Origin times and locations are from Marshall, Bache and Lilwall (1984). m_b values are from Dermengian, Murphy and Barker (1985).

thus, support the hypothesis that they are associated with variations in the near-source P wave propagation paths to teleseismic distances (Barker and Murphy, 1986). As reported by Dermengian et al. (1985), attempts to determine the magnitude of the variation in selected azimuth windows were inconclusive due to the possibility of network magnitude bias caused by azimuthal clustering of stations for most of the explosions. Thus, while the differences between the m_b patterns for pairs of events could be well constrained, the absolute value of the residual change in any one azimuth was indeterminate.

2.2 ESTIMATION OF UNBIASED NETWORK-AVERAGED m_b VALUES

In order to develop a method of obtaining unbiased estimates for the event magnitudes from which accurate single station m_b residuals can be computed, we have examined the correlation structure of the set of station-corrected m_b residuals calculated in Dermengian et al. (1985). These prior results were based on network m_b averages computed from stations which were geographically clustered and correlated to some degree, resulting in the possibility of biased network m_b values. In order to first determine the degree to which the single station m_b residuals were correlated, station-station m_b residual correlations were computed for all station pairs in the dataset. To first order, station-station correlation is a complicated function of the separation between stations on the focal sphere, with the smoothness of the function varying depending on the geographical location of the stations. An example of the effect of geographical proximity on the correlations between station residuals can be seen in Figure 2, which shows the population of station-station correlation coefficients for a group of 18 stations located in France. For this group of stations, which have a mean separation of a few hundred kilometers, the station-station correlations are largely positive. It follows from this figure that if station-corrected m_b values at a station in France are biased high or low relative to a worldwide network average then, to a certain degree the other stations in France will be biased in the same manner. Alternately, using single station m_b values recorded by this group of stations in the determination of a network m_b can result in biased network m_b values if simple averaging is used.

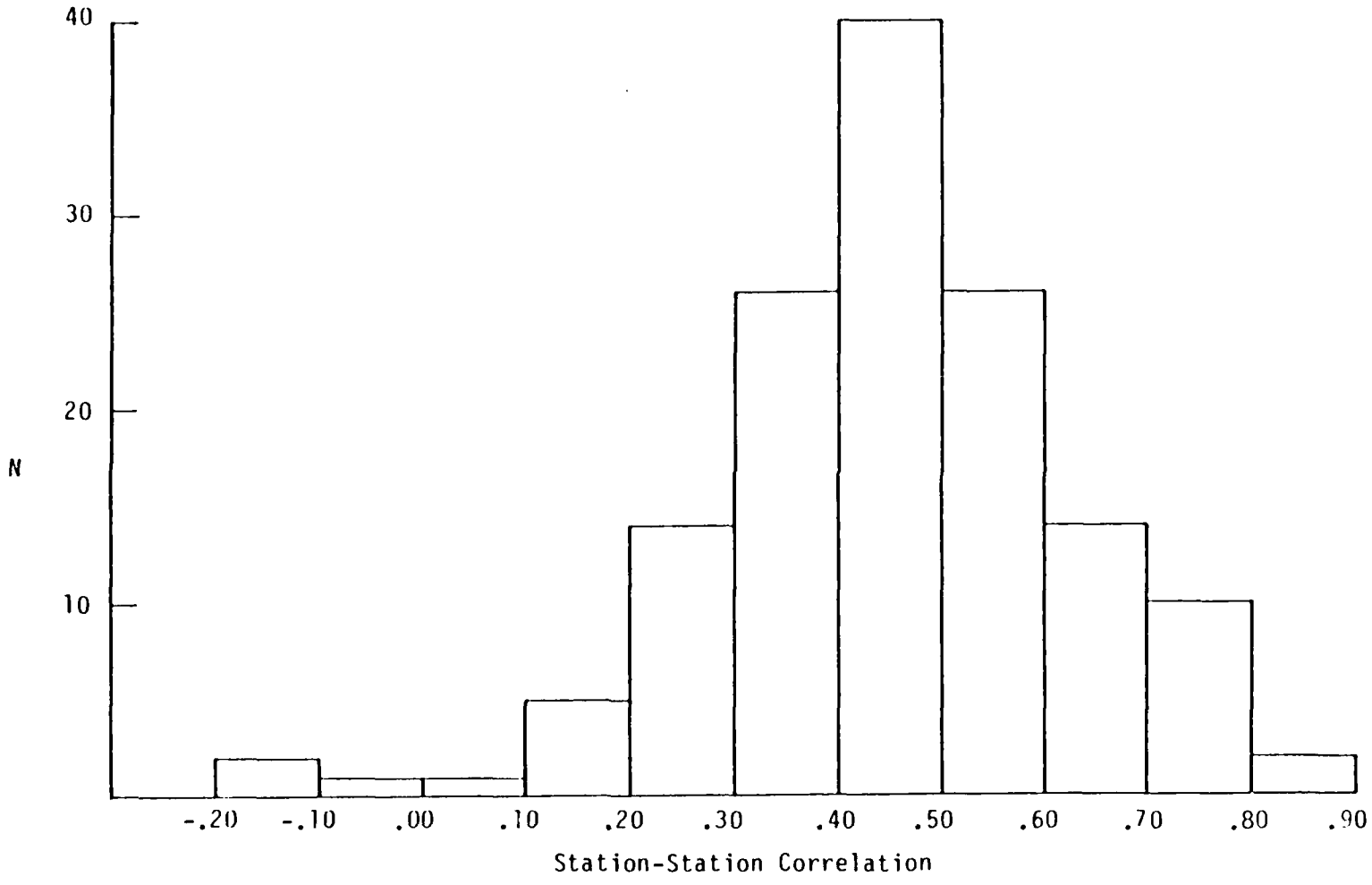

Figure 2. Histogram showing the population of station-station correlation coefficients for 18 stations in France.

In order to account for this potential biasing effect of station-station correlation we developed an ad hoc scheme whereby stations which were highly correlated would be given appropriately less weight in the averaging process. By using the station-station correlations as a clustering variable, the majority of the stations in our dataset can be placed in one of three groups such that the within-group station-station correlations are predominantly positive. These three groups are (1) stations in North America, (2) stations in continental Europe less than 45 degrees distance from Shagan River, and (3) stations in France. When station-station correlations for station pairs within each of the three groups are examined in more detail on an individual basis there are certain sub-groups of stations which appear to account for most of the large-positive correlations observed, these correlations being generally greater than 0.5. Other stations in the groups contribute most to the correlations which are positive but not as large as 0.5. To account for this, stations were re-grouped into smaller groups such that station-station correlations for pairs of stations in the same group were predominantly large and positive. The remaining stations were considered as independent. Then, for each event in our dataset, a revised m_b was computed by averaging within each group and then computing a final average of the group values with the values reported by the independent stations.

Figure 3 shows how the revised event magnitudes compare with the original values computed by the least squares analysis of Dermengian et al. (1985) as a function of event location. It can be seen in this figure that for the majority of the events the adjustments caused by the new averaging procedures are quite small, with around 60 percent of them being less than or equal to 0.08 magnitude units in absolute value. There are a few events, however, where the adjustments are more substantial, and these seem to be concentrated in the central and northeast portions of the test site where the most pronounced residual variation with azimuth is observed. Thus, it appears that the process of grouping stations based on their inter-station correlations has resulted in relatively minor adjustments to the majority of the network m_b values

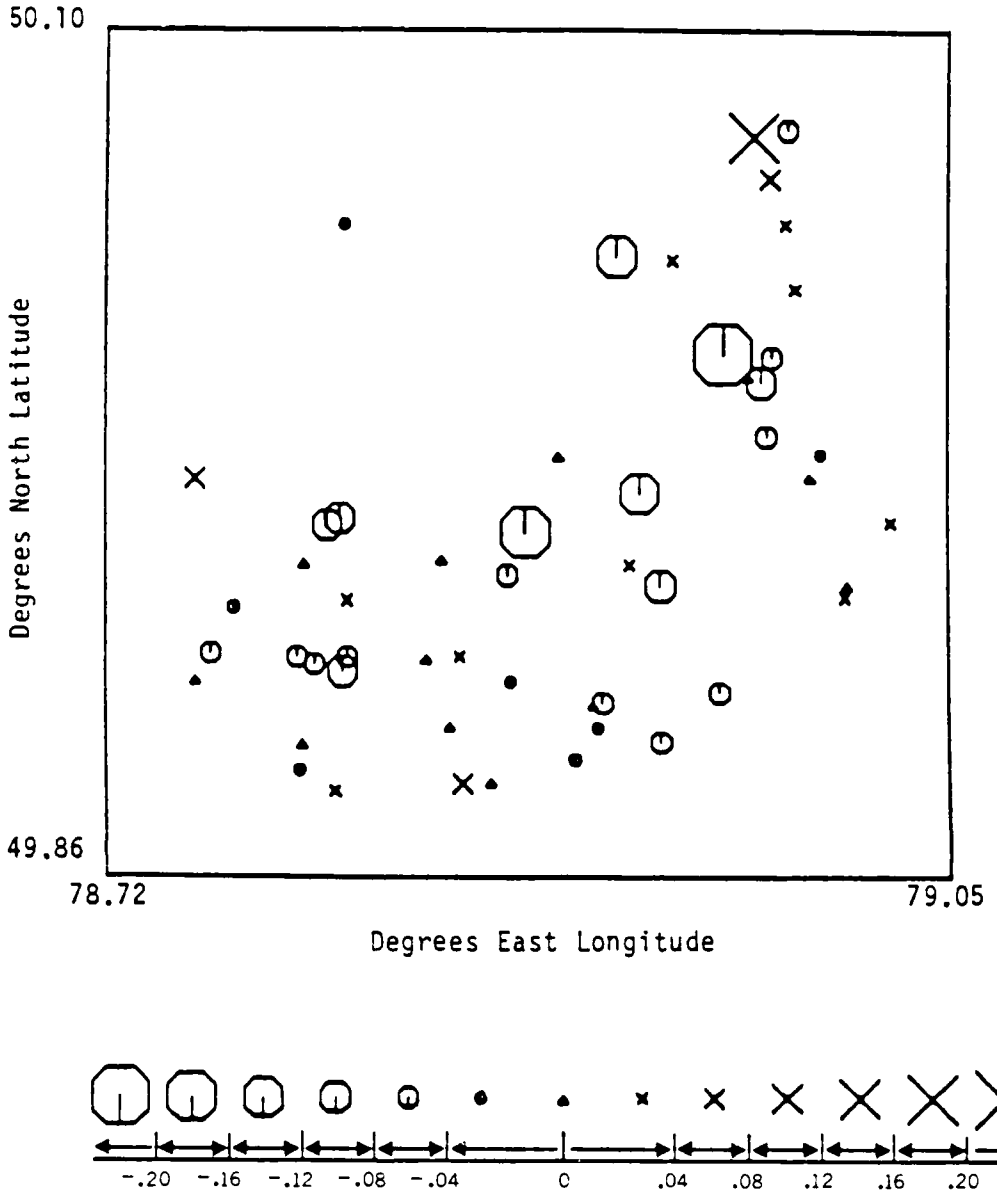

Figure 3. Differences between revised event magnitudes of this report and those of Dermengian et al. (1985), as a function of event location.

previously calculated using a least squares technique, particularly for events in the southwest portion of the test site. For a few of the events, notably some of the central and northeastern events, the adjustments are more substantial. We will now investigate the effect that application of these adjustments has on some of the more important results obtained by Dermengian et al. (1985).

2.3 m_b RESIDUAL ANALYSIS

Using the revised network m_b values obtained above, we have re-computed single station m_b residuals for all station-event pairs in the dataset. As in the original study of Dermengian et al. (1985), these revised data provide evidence of some unaccounted for source region physical mechanisms which are affecting the radiation of P wave energy to teleseismic distances. This is illustrated in Figure 4, which shows the station-corrected m_b residuals as a function of event location for station ALE in Canada and station HFS in Sweden. Note that the residuals, which can be regarded as variations in the "station corrections" with source location, show pronounced trends in that residuals of the same size and sign tend to cluster into geographical groups. Now in Dermengian et al. (1985), an attempt was made to group stations which appeared to be highly correlated and average their residual patterns as a function of source location, with the aim of contouring the mean m_b residuals across the test site. In that report, the station grouping was based on visual comparisons of plots of station data. Using more precise information obtained from our correlation analysis, we have re-grouped the stations and performed a similar analysis. Eleven stations in North America having generally positive station-station correlation were selected as the first group. For each event in the dataset, the m_b residuals at those stations in the group which recorded the event were averaged. The residuals as a function of event location computed using these 11 stations in North America is shown in Figure 5. In this, and subsequent plots of the same kind, rough contour lines have been drawn to highlight the general trends. As Dermengian et al. (1985) showed for a smaller

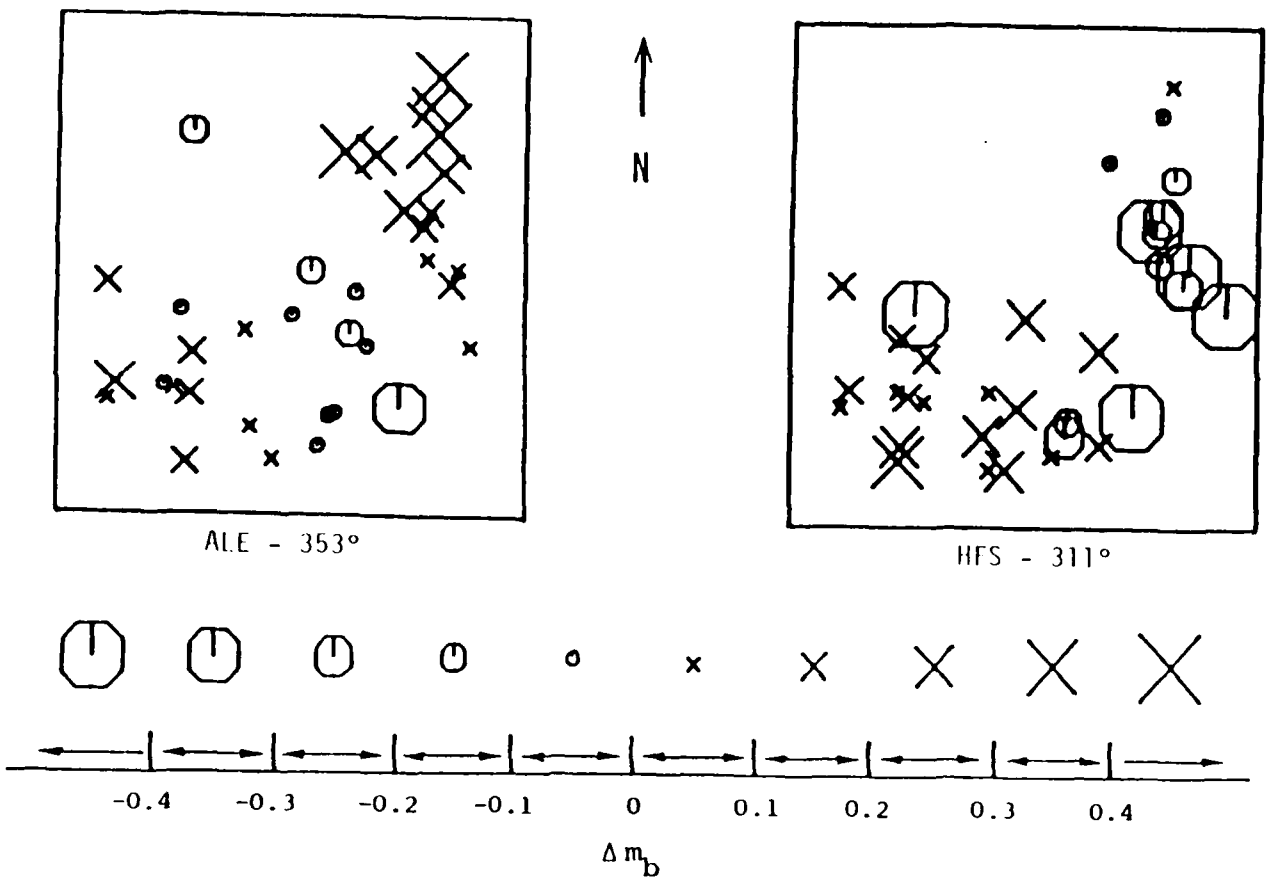

Figure 4. Station-corrected m_b residuals as a function of event location for station ALE in Canada and station HFS in Sweden at the denoted recording azimuths.

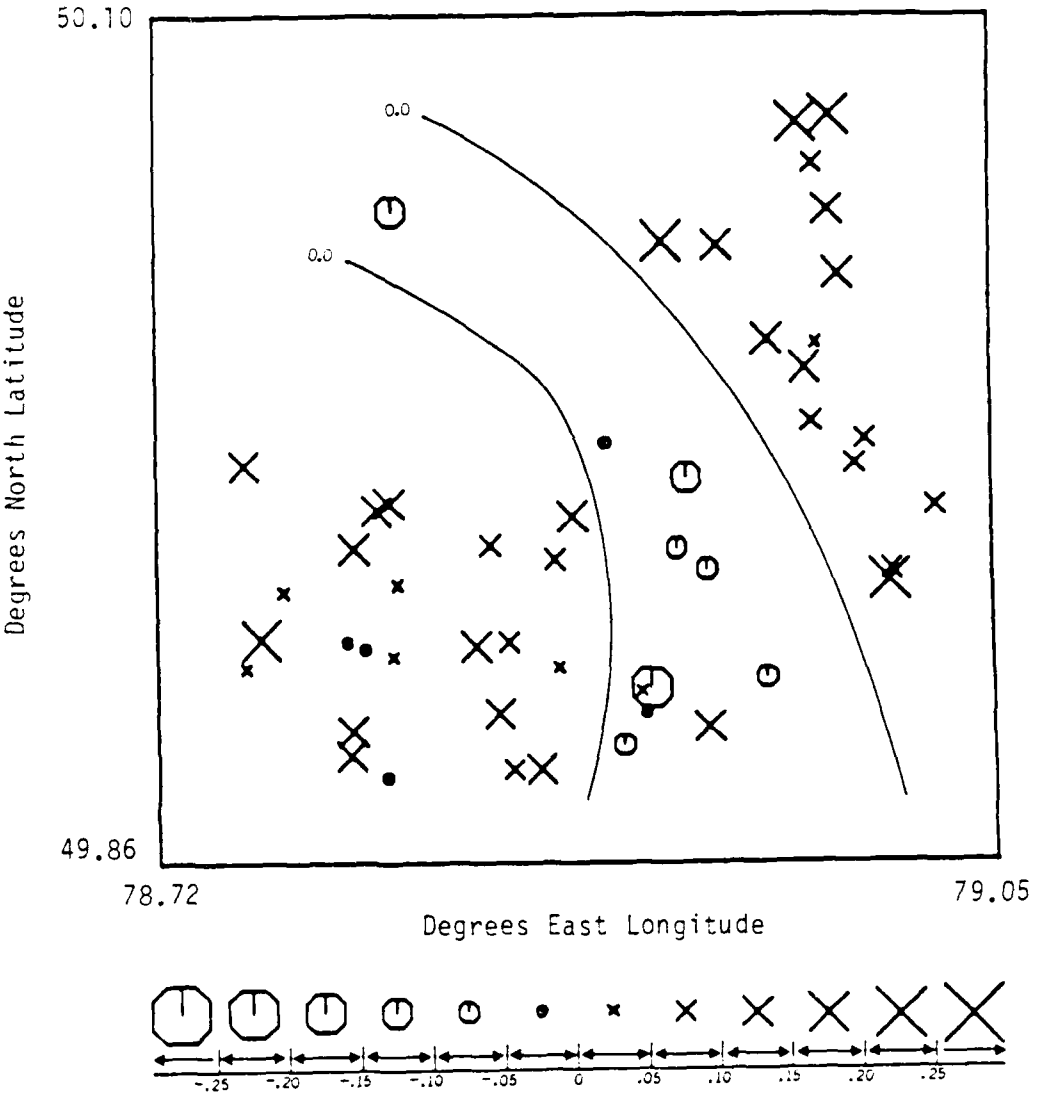

Figure 5. Contours of mean m_b residuals across the Shagan River test site derived from a group of 11 stations in North America.

group of stations in the same area, the average station-corrected m_b residuals for events in the northeast and central portions of the test site are relatively large and vary by a few tenths magnitude units over this area. Specifically, North American stations see events in the northeast portion of the test site as being larger than the worldwide average and events in the central portion as being smaller than the worldwide average. A similar plot for a group of 17 French stations which were determined to be highly correlated is shown in Figure 6. The variation in the average station-corrected m_b residuals as a function of event location for these stations is also fairly regular and even larger, although opposite in sign, than that shown for the stations in North America. As mentioned earlier in this section, a third group of stations which were found to have generally positive station-station correlations consists of stations in continental Europe at epicentral distances of less than 45 degrees from the Shagan River test area. A similar plot for this group of stations is shown in Figure 7. In this figure, it can be seen that the sign of the variation in the northeast and central areas of the test site is the same as for the French stations, although the magnitude of the variation for this group of stations is less than both the French stations and the North American stations. Thus, these figures present further evidence that the variations in m_b residuals for stations in a given azimuth and distance range are systematic enough that they can be contoured as a function of source location. This result supports the hypothesis that the observed differences are associated with changes in the near-source P wave propagation paths to teleseismic distances as a function of source location within the test site. Moreover, the extent of the variation appears to vary with the geographic location of the stations, with stations in France showing the largest amount of variation over the smallest source region area.

A better way of illustrating these variations in m_b residual patterns is by comparing corrected m_b residuals for different pairs of events at common sets of stations. Figures 8 and 9 show four such comparisons for pairs of events located in the central/northeast region of the test site, the area which shows the largest variation with source location at the stations in France. In each of these figures the stations are grouped by geographic location in order to highlight the differ-

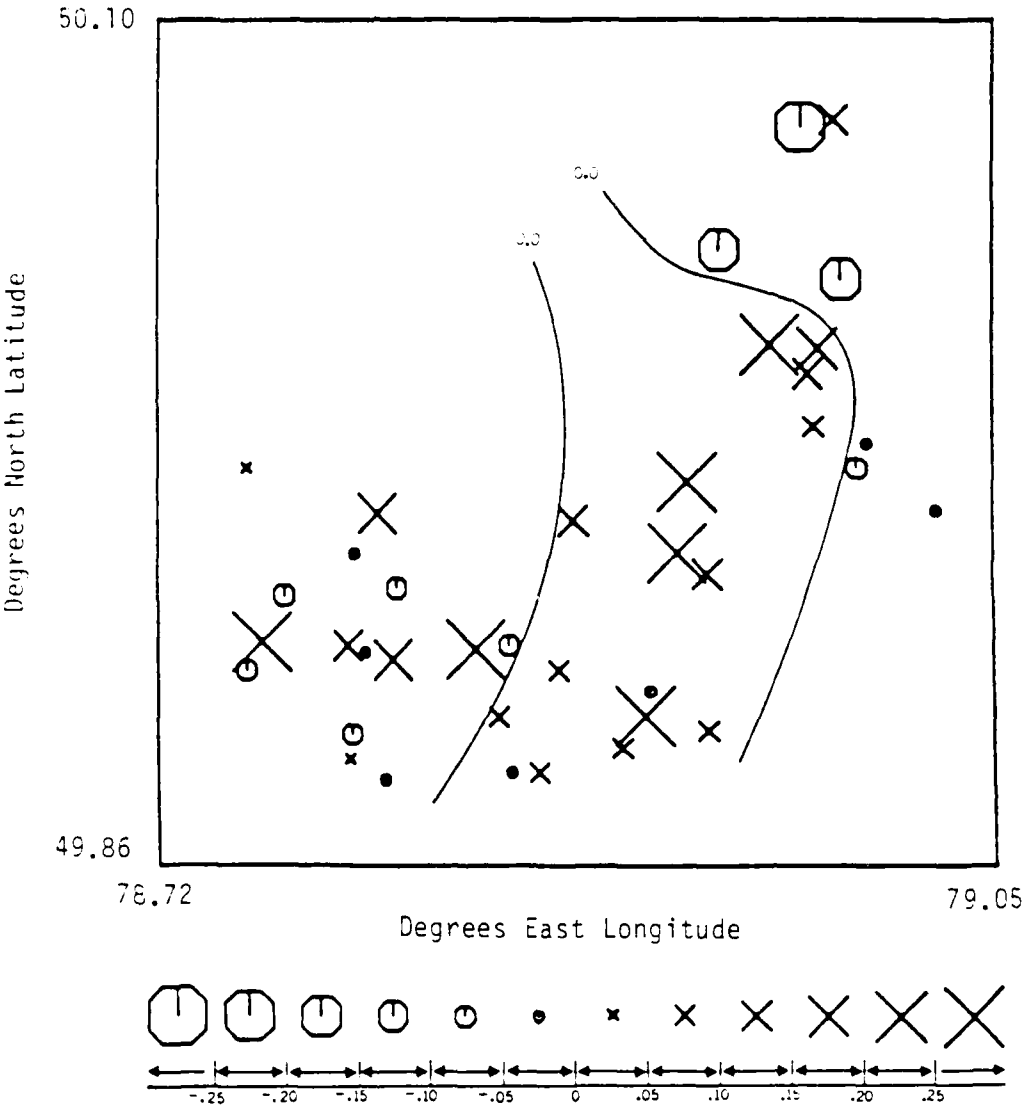

Figure 6. Contours of mean m_b residuals across the Shagan River test site derived from a group of 17 stations in France.

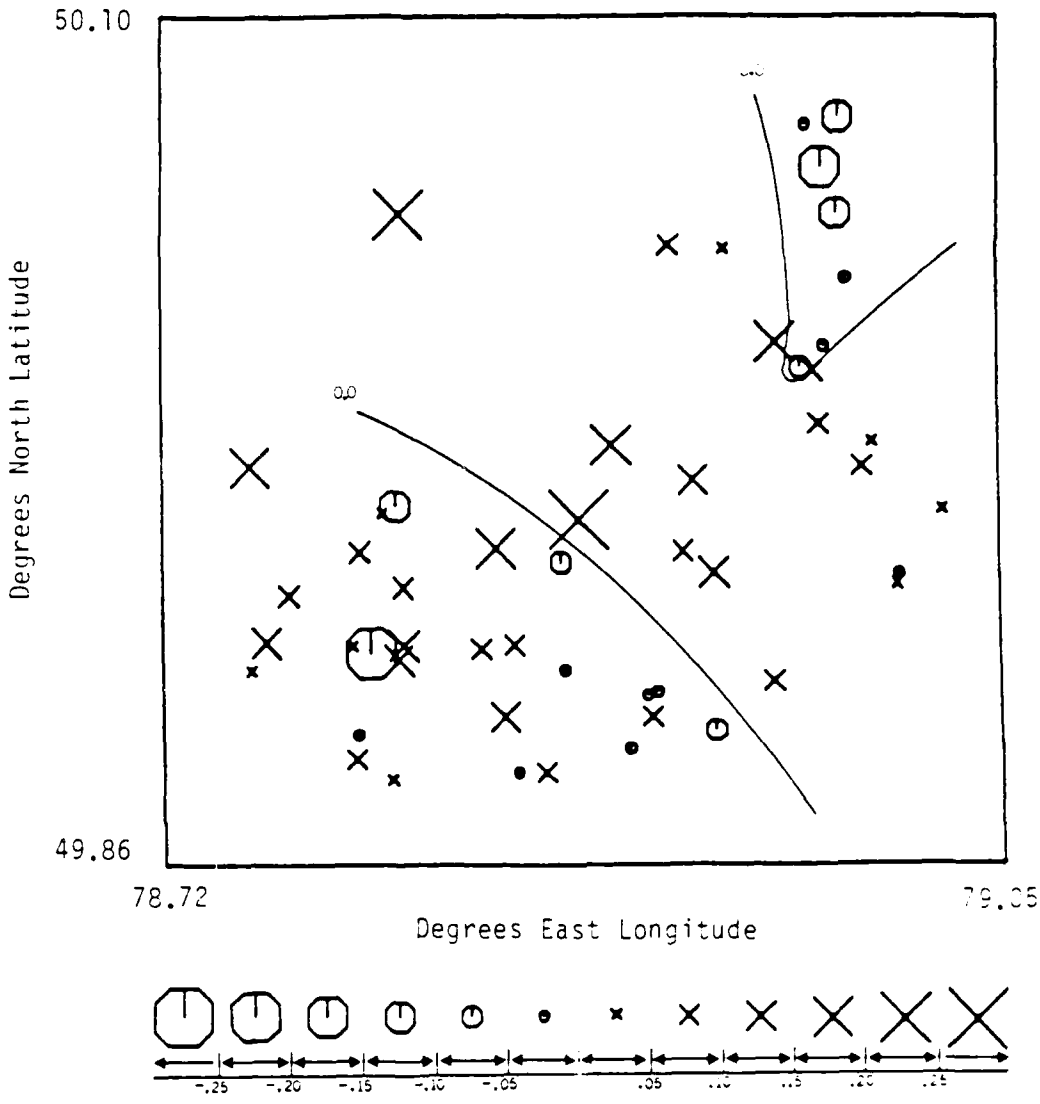

Figure 7. Contours of mean m_b residuals across the Shagan River test site derived from a group of eight stations in Europe at less than 45 degrees distance.

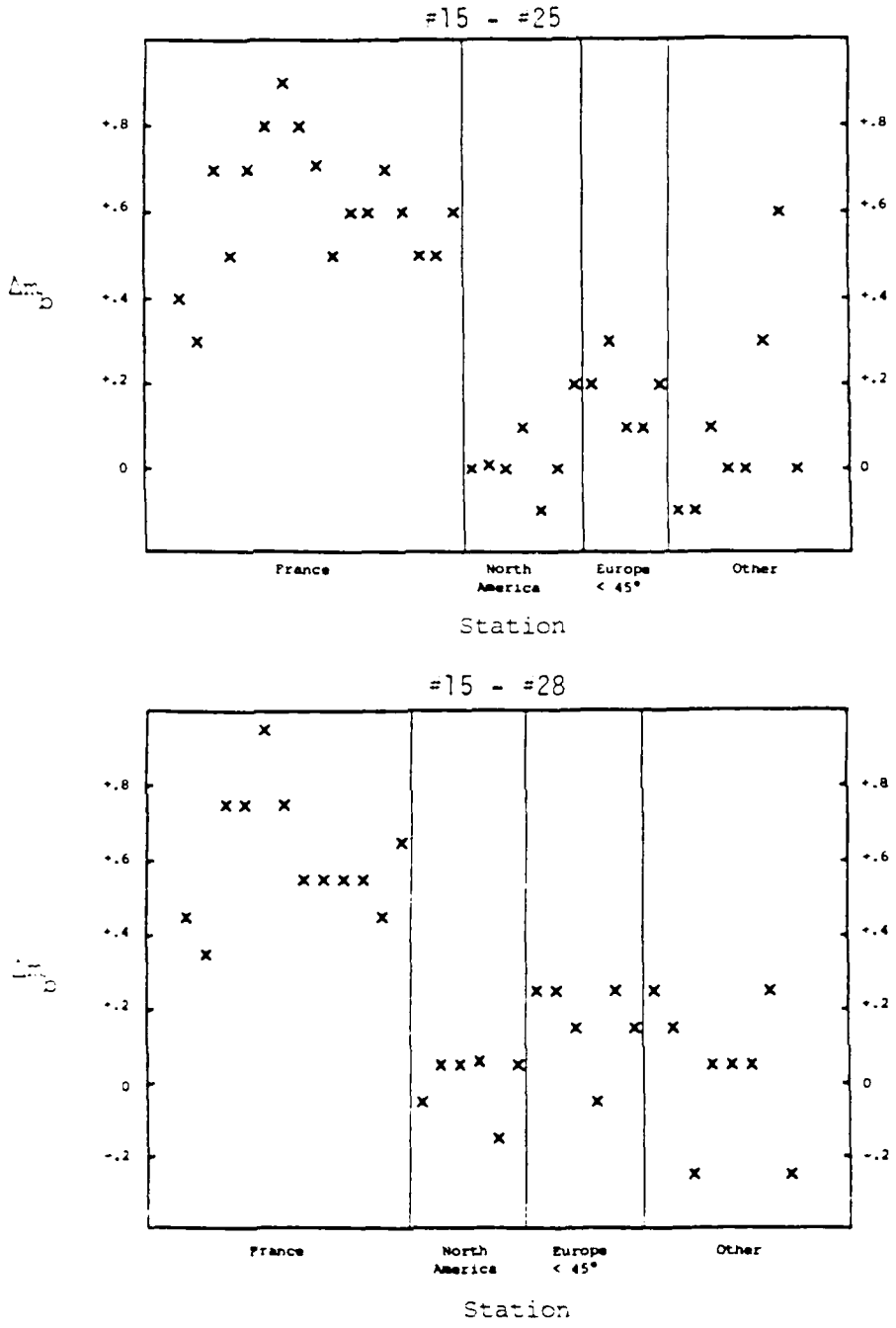

Figure 8. Station-corrected m_b residual differences between event #15 and events #25 and #28 as a function of station location.

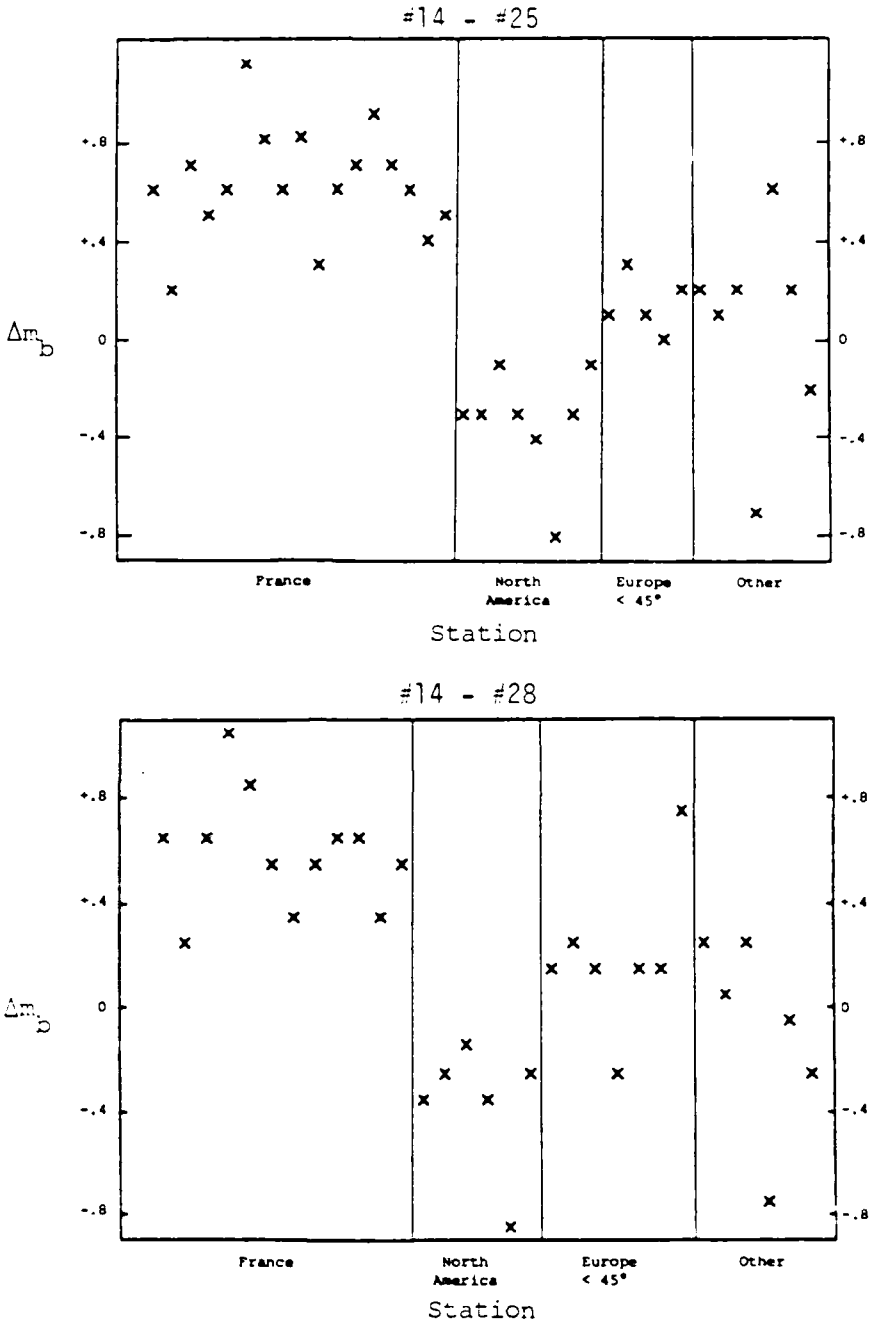

Figure 9. Station-corrected m_b residual differences between event #14 and events #25 and #28 as a function of station location.

ences between the station groups that was seen in Figures 5 through 7. As Figure 8 shows, the residuals seen by the French stations for event #15 differ greatly from those seen by the same stations for events #25 and #28, which are located only a few kilometers away. These differences can amount to over 0.8 magnitude units in some cases. Stations in Europe less than 45 degrees distance from the test area also see differences between the pairs of events, although these differences are not nearly as large as those seen by the French stations. Stations in North America, along with most of the other remaining stations, see generally random residual differences for these event pairs. A somewhat different picture emerges in Figure 9, however. Here we show residual comparisons between event #14, located a little nearer to the center of the test site, and the same two events #25 and #28. In this case, the differences seen by the French and other European stations are much the same as was shown in Figure 8. The North American stations, however, now see smaller residuals for event #14 than they see for events #25 and #28. The other remaining stations, once again, see a more random pattern of differences. These variations are quite consistent with the general trends shown in the contour plots of Figures 5 through 7, confirming the fact that large variations in corrected m_b residuals do occur between events in close proximity in the northeast and central portions of the Shagan River test site. Moreover, these variations not only appear to have a dependence on station azimuth, as evidenced by the differences between the French and North American stations, but they also appear to have a dependence on take-off angle. Evidence of this is given by the differences seen between the French stations and the other European stations which lie along essentially the same azimuths but have different take-off angles from the test area.

This variation in the m_b residuals as a function of take-off angle to the French and European stations is illustrated more clearly in Figure 10 which shows the focal sphere projections of the residuals observed at these stations for the four closely-spaced events #15, #25, #28 and #41 (cf. Figure 1). It can be seen that for events #15 and #41, the m_b residuals at stations in France (take-off angles less than the 26° indicated by the dashed lines) have large positive residuals while

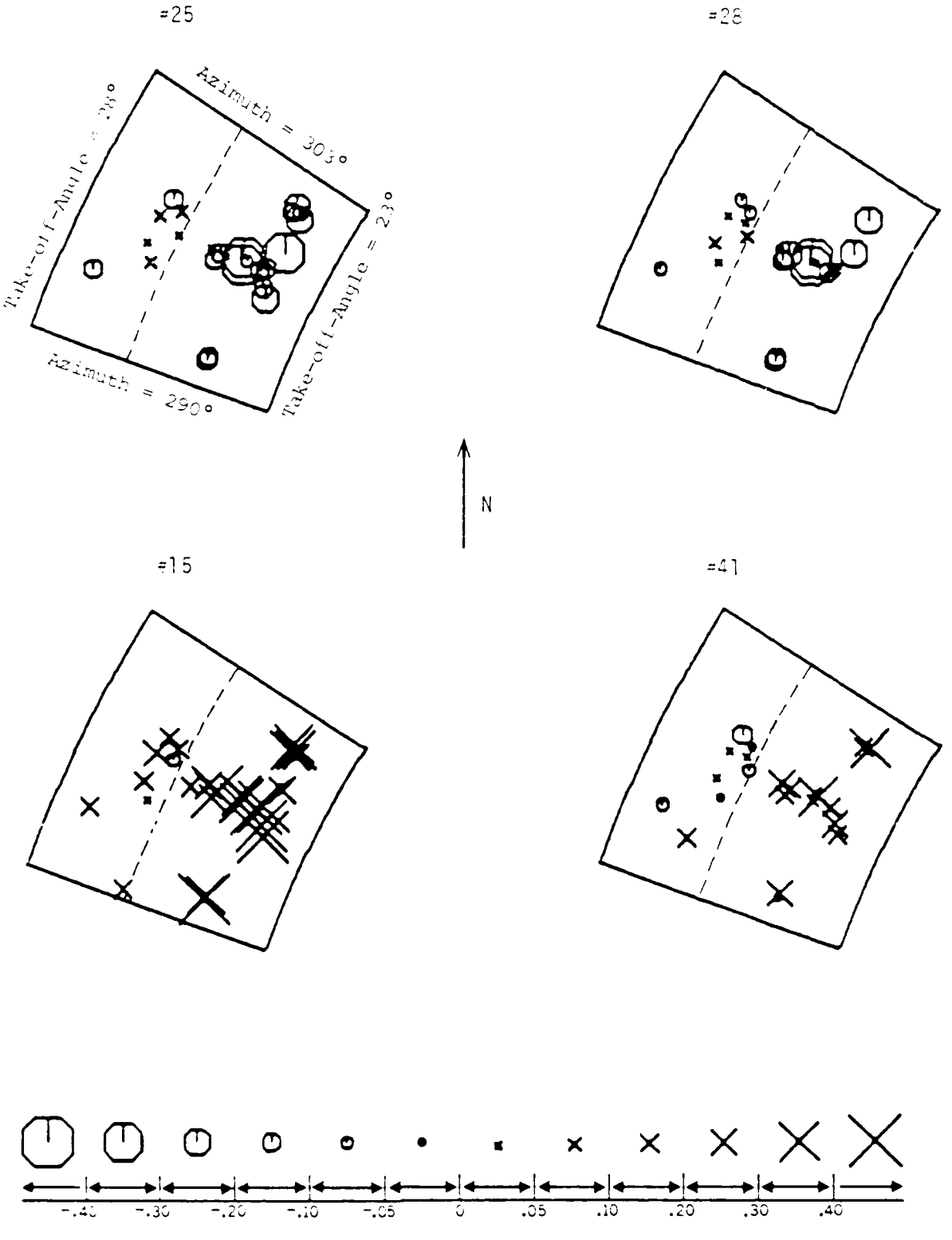

Figure 10. Focal sphere projections of the m_b residuals at stations in Europe for events #15, #25, #28 and #41.

those for the other stations in Europe (take-off angles greater than 26°) average close to zero. For events #25 and #28, on the other hand, the French stations show large negative residuals, while the nearer European stations again show small residuals which average close to zero. Thus, the principal variations in m_b as a function of source location are occurring at the French stations, which suggests that the P waves leaving the source region through the corresponding portion of the focal sphere are encountering some anomaly in the subsurface structure beneath the Shagan River test site.

2.4 PRELIMINARY EVALUATION OF THE SOURCE OF THE m_b ANOMALY

In order to gain some insight into the cause of the observed m_b anomalies at the French stations, a first order ray trace analysis has been conducted in which the m_b residuals for the four events of Figure 10 have been projected onto planar surfaces at different depths using the known azimuths and ray parameters to the European stations of interest. Figure 11 shows the approximate surface projections of the illuminated areas as a function of depth with respect to the location of the Shagan River test area. Figures 12 through 14 show the projections of the m_b residuals for the four events on six depth slices spaced 25 km apart between 25 and 150 km depth. It can be seen that at shallow depths (cf. Figure 12), the large negative and positive residuals (large circles and x's, respectively) are strung out in a linear fashion and heavily intermingled with normal values with residuals close to zero. Clearly such a pattern is not consistent with a confined, geometrically regular source of the m_b anomaly. However, at the intermediate depths (cf. Figure 13) the large negative and positive residuals begin to cluster into groups, until at around 100 km almost all the large negative residuals have coalesced into the northeast quadrant of the projected plane. At still deeper depths (cf. Figure 14), the large positive and negative residuals begin to intermingle again, suggesting that the P waves to these stations are encountering an anomalous volume of material at depths between about 75 and 125 km.

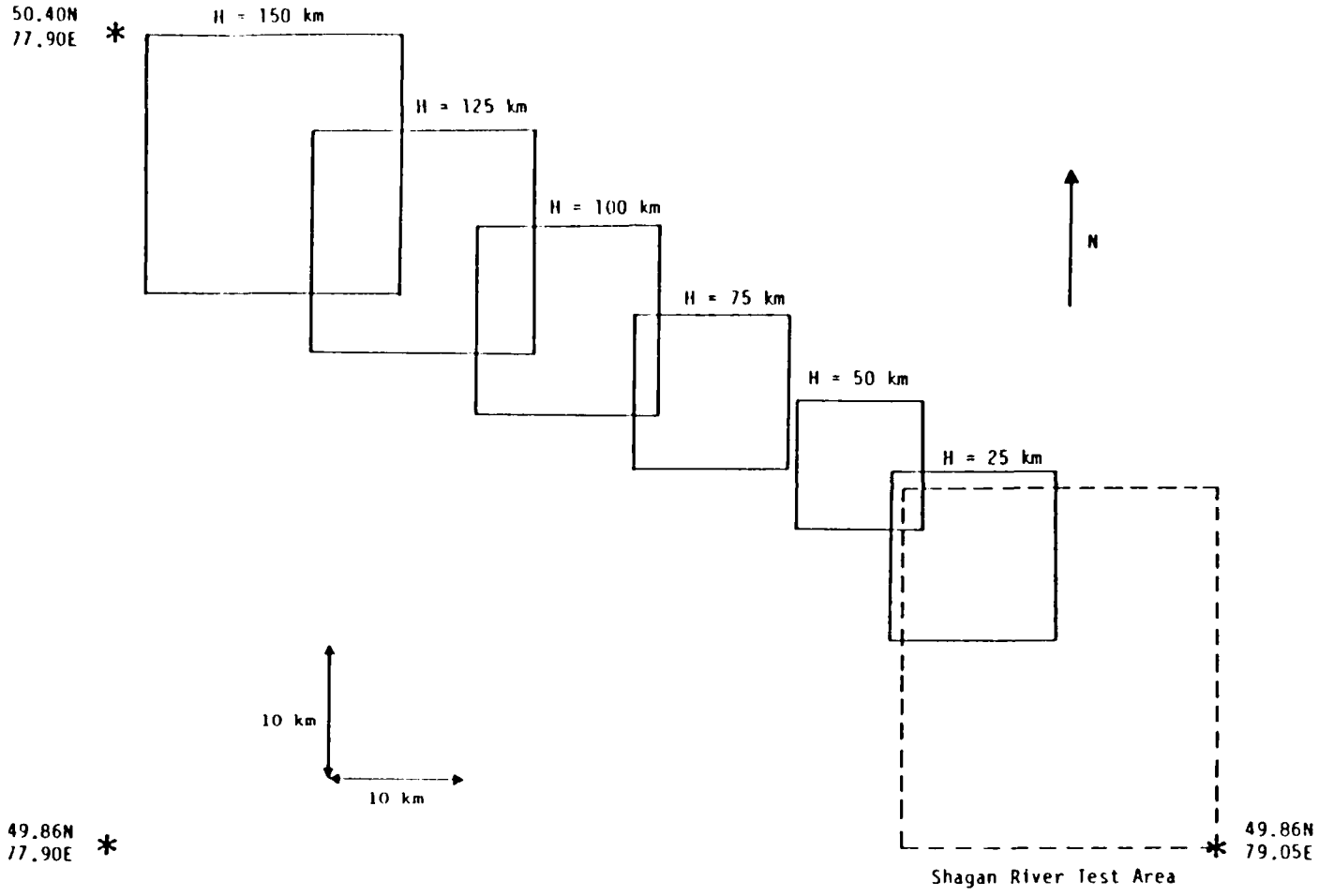

Figure 11. Approximate surface projections of the areas illuminated by the ray trace analysis.

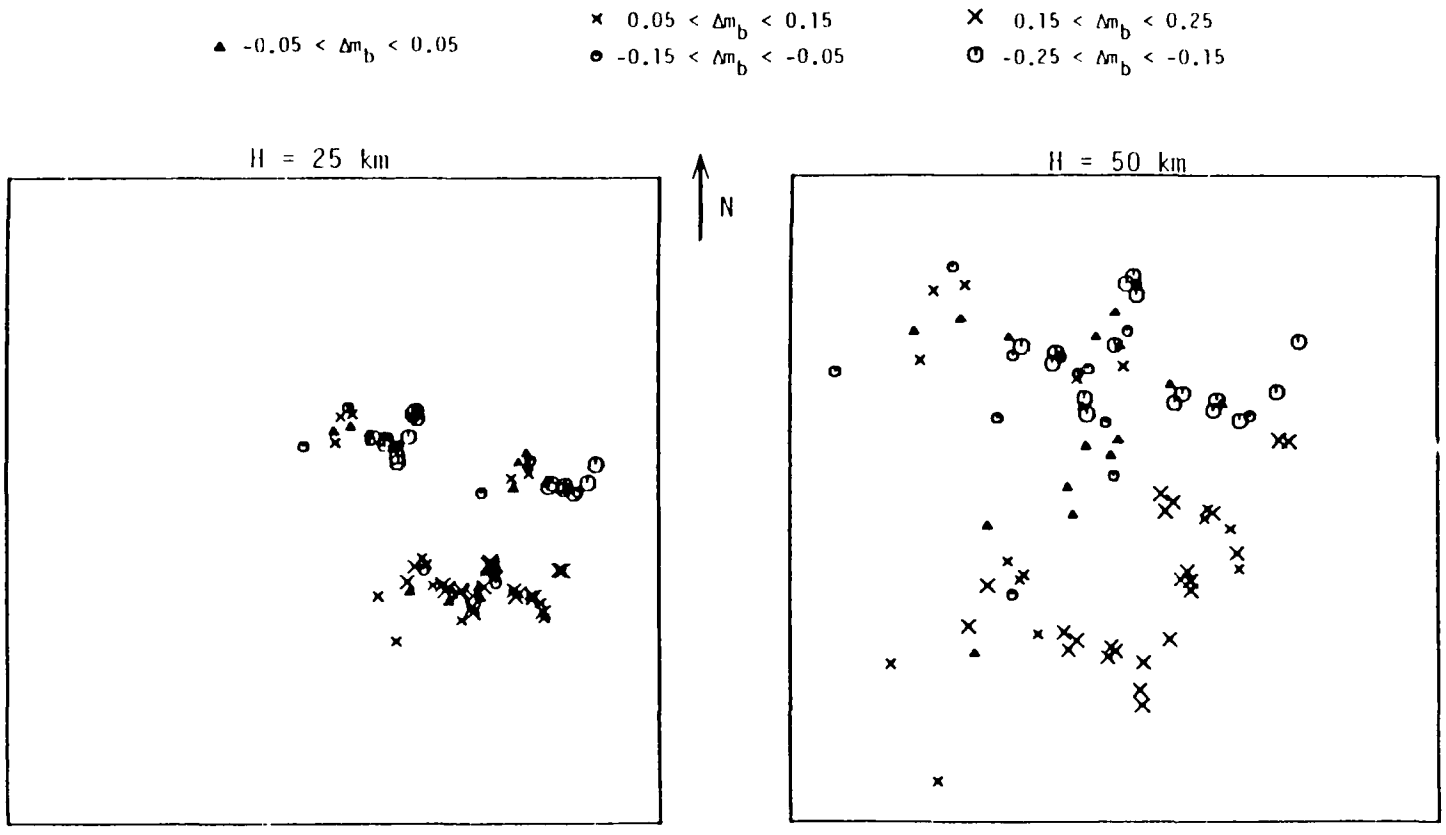

Figure 12. Projections of the m_b residuals for four events at depths of 25 km and 50 km.

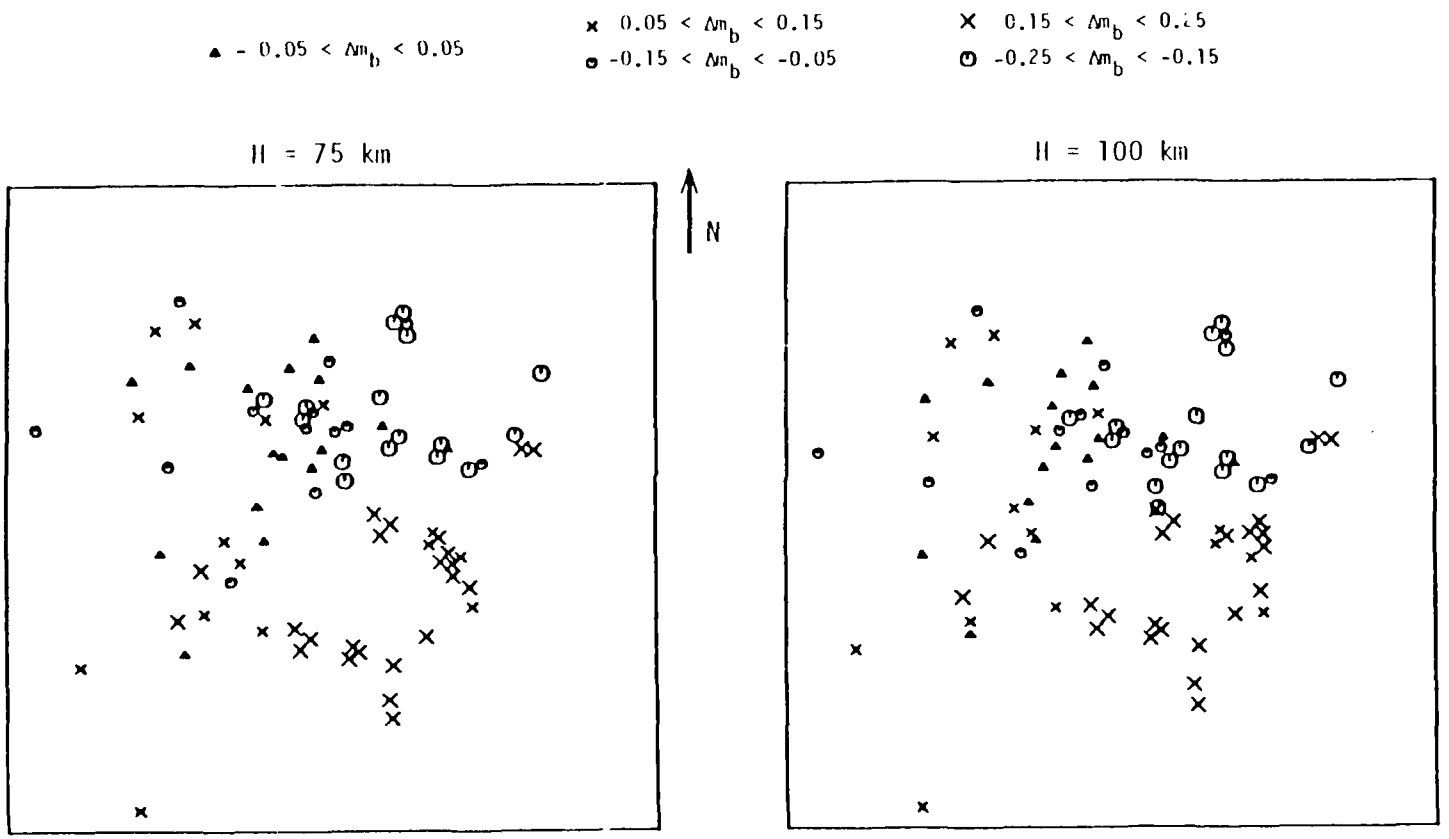

Figure 13. Projections of the m_b residuals for four events at depths of 75 km and 100 km.

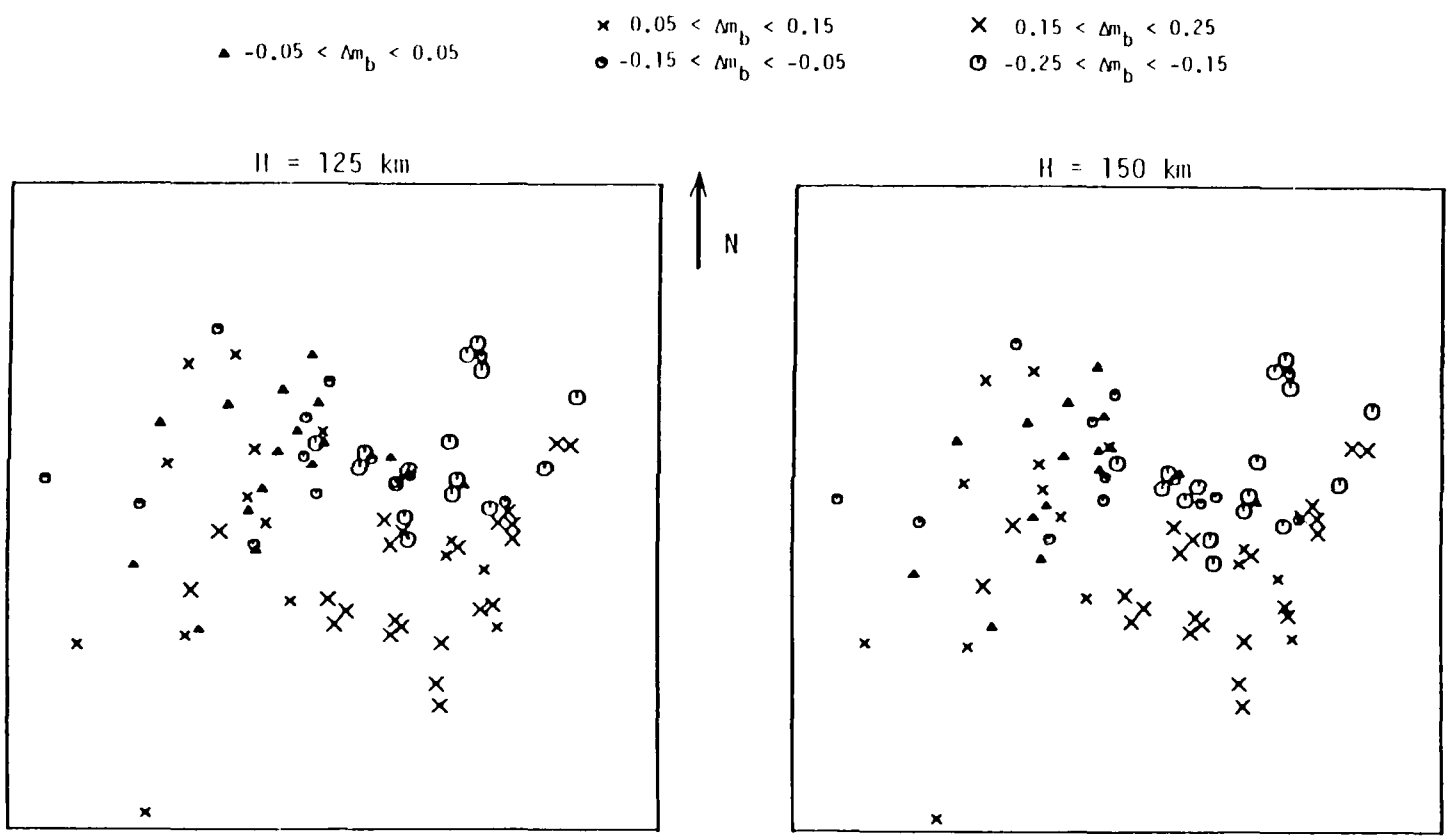

Figure 14. Projections of the m_b residuals for four events at depths of 125 km and 150 km.

In order to examine the geometry of the anomalous volume in more detail, m_b residuals at these same stations from five additional events in the same general area of the test site were added to the analysis. The locations of all nine events are shown in Figure 15. Figures 16 through 18 show the projections of the m_b residuals for the nine events on the same six depth slices shown in Figures 12 through 14. These additional data show very much the same patterns as the original four events and provide somewhat better spatial resolution. Once again the large negative residuals appear to coalesce into a homogeneous group in the northeast quadrant at a depth of about 100 km. The nine event residual pattern at a depth of 100 km is reproduced in Figure 19, where rough boundaries have been sketched in to encompass areas of predominantly large negative (solid line) and positive (dashed line) residuals. It can be seen that this rough partition captures almost all the large negative residuals in a homogeneous group containing no positive residuals and only two near-zero residuals. Similarly, the dashed line encloses most of the large positive residuals with no negative residuals and a relatively small percentage of normal (i.e. near-zero) values.

The extent to which the partitioning of Figure 19 separates the four event residuals is shown in the left panel of Figure 20. It fits these data well, particularly the rather sharp western boundary which defines the extent of the large negative residuals as suggested by the data from the four events alone. The right hand panel of this figure shows the residuals for the nine events at the same 100 km depth for four French stations selected to illustrate the consistent changes in the m_b residuals with source location from normal to large positive to large negative as the station projections migrate from south to north across this section.

Figure 21 shows the nine event m_b residuals at 100 km depth from Figure 19, split into two groups of stations. The left panel shows the nine event residuals for the 15 stations which contribute large negative residuals to the northeast cluster of data. The panel on the right shows the nine event residuals for the remaining nine stations. It can be seen from the left panel that the residual data from the 15 stations

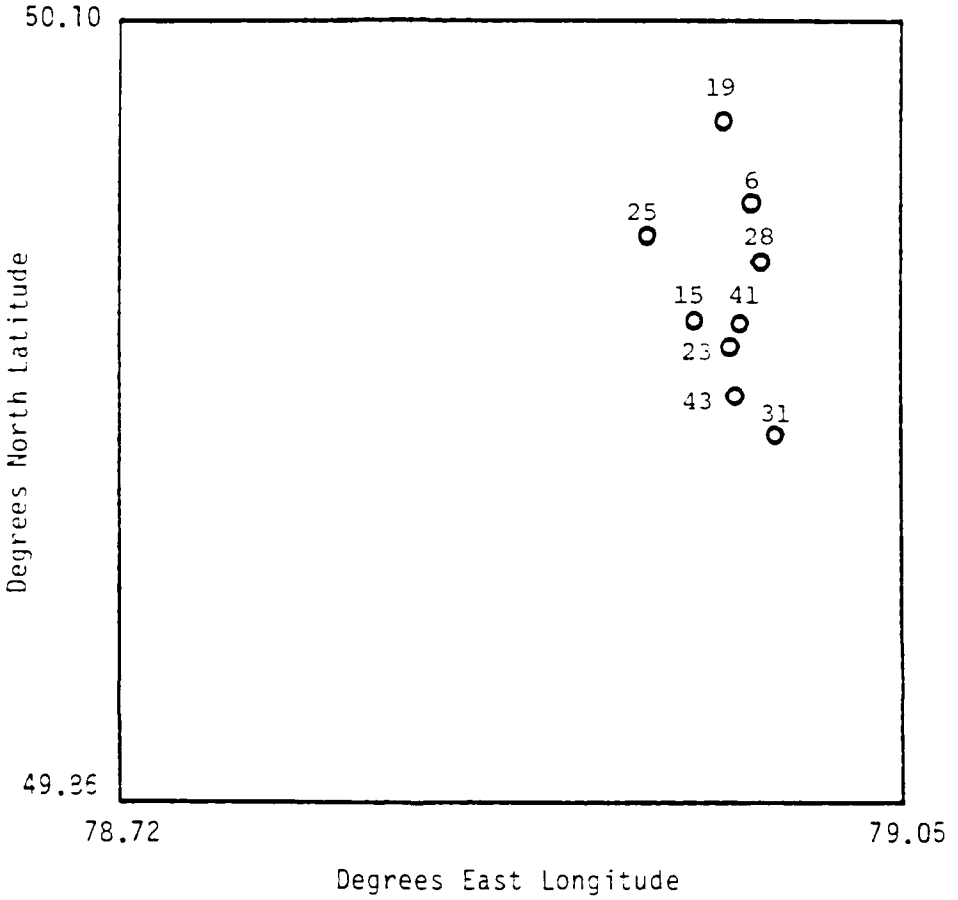

Figure 15. Locations of the nine events used in the ray trace analysis.

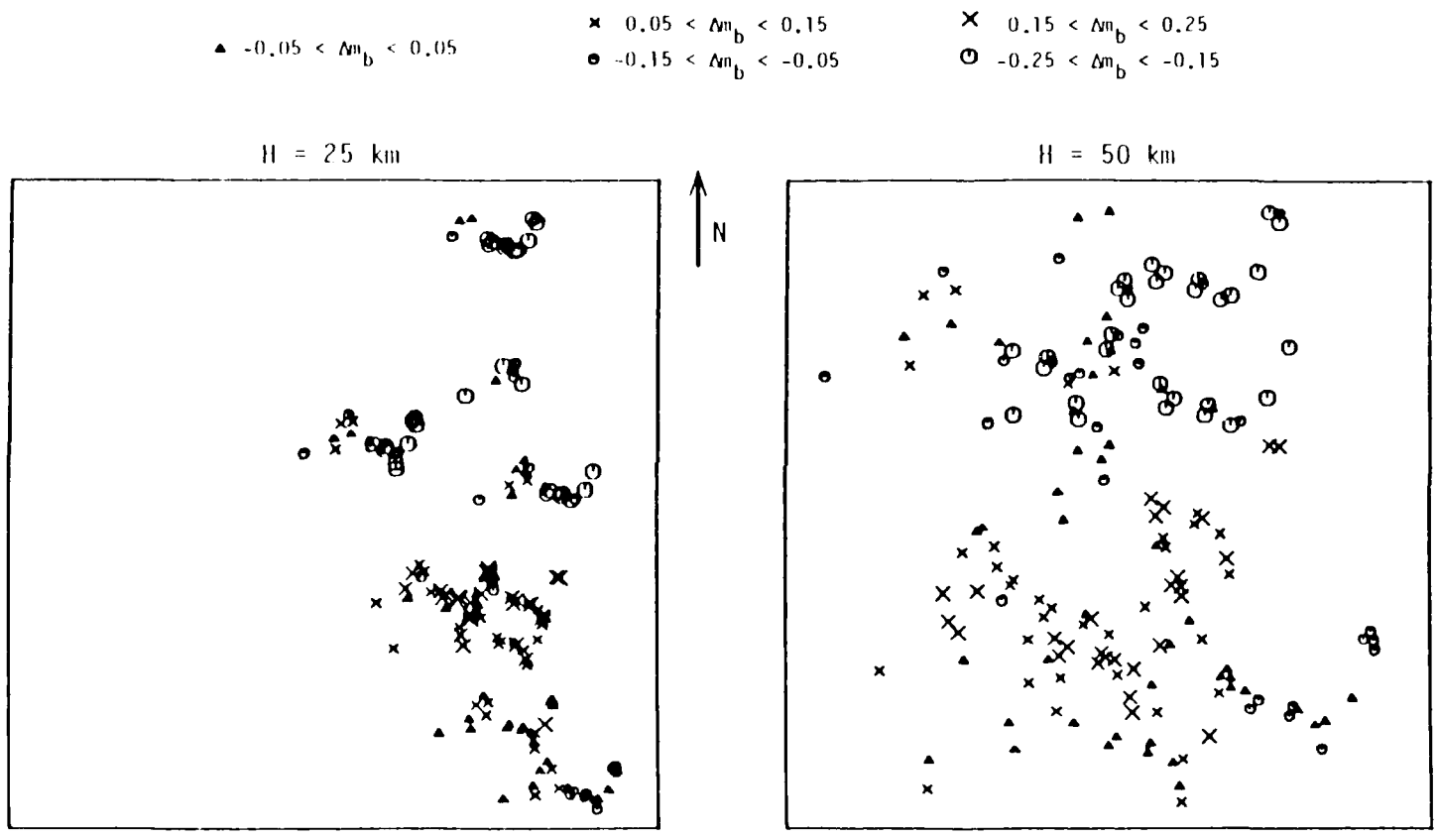

Figure 16. Projections of the m_b residuals for nine events at depths of 25 km and 50 km.

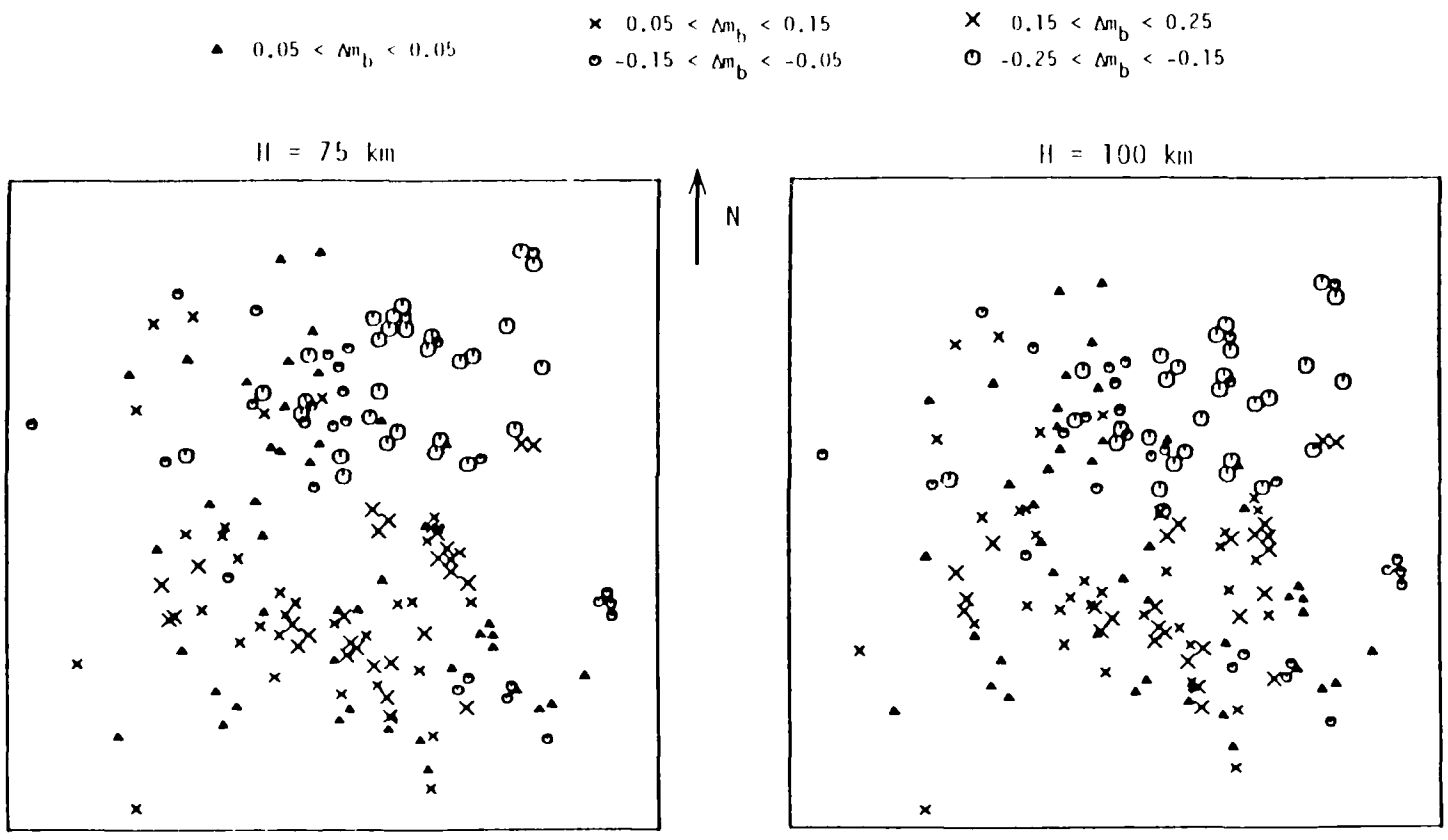

Figure 17. Projections of the m_b residuals for nine events at depths of 75 km and 100 km.

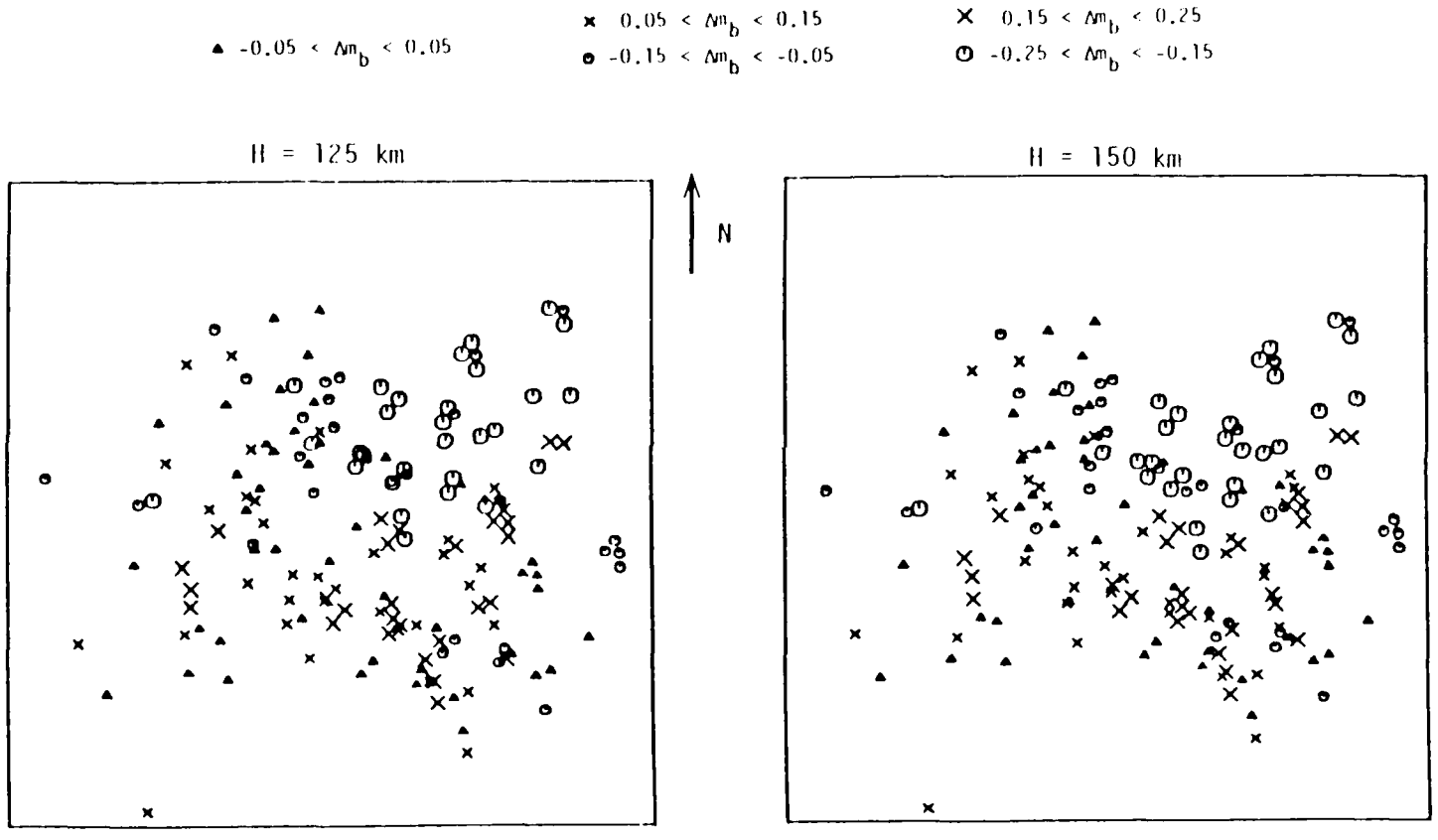

Figure 18. Projections of the m_b residuals for nine events at depths of 125 km and 150 km.

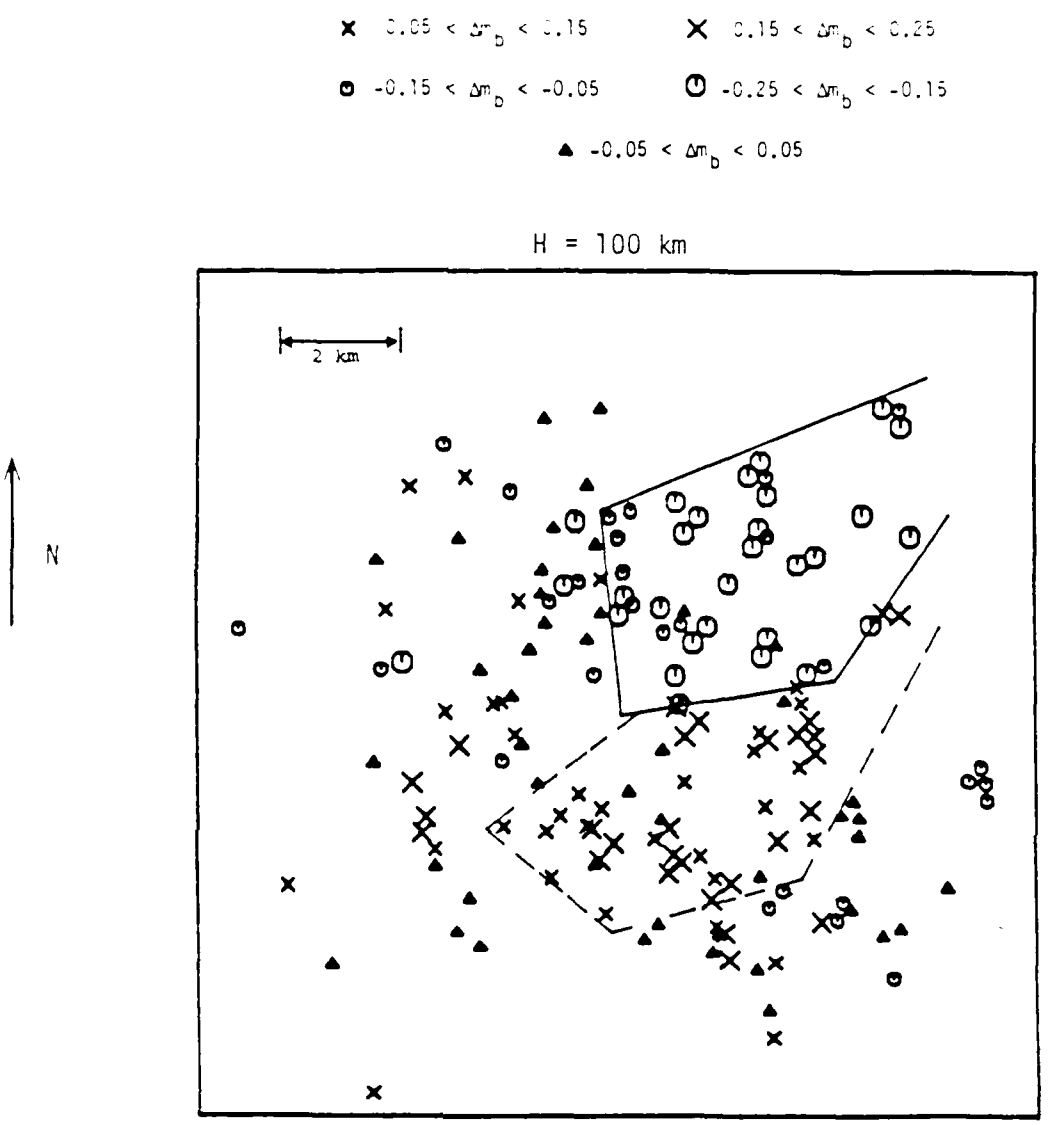

Figure 19. Nine event residual patterns at a depth of 100 km, showing boundaries sketched in to encompass areas of predominantly large negative (solid line) and large positive (dashed line) residuals.

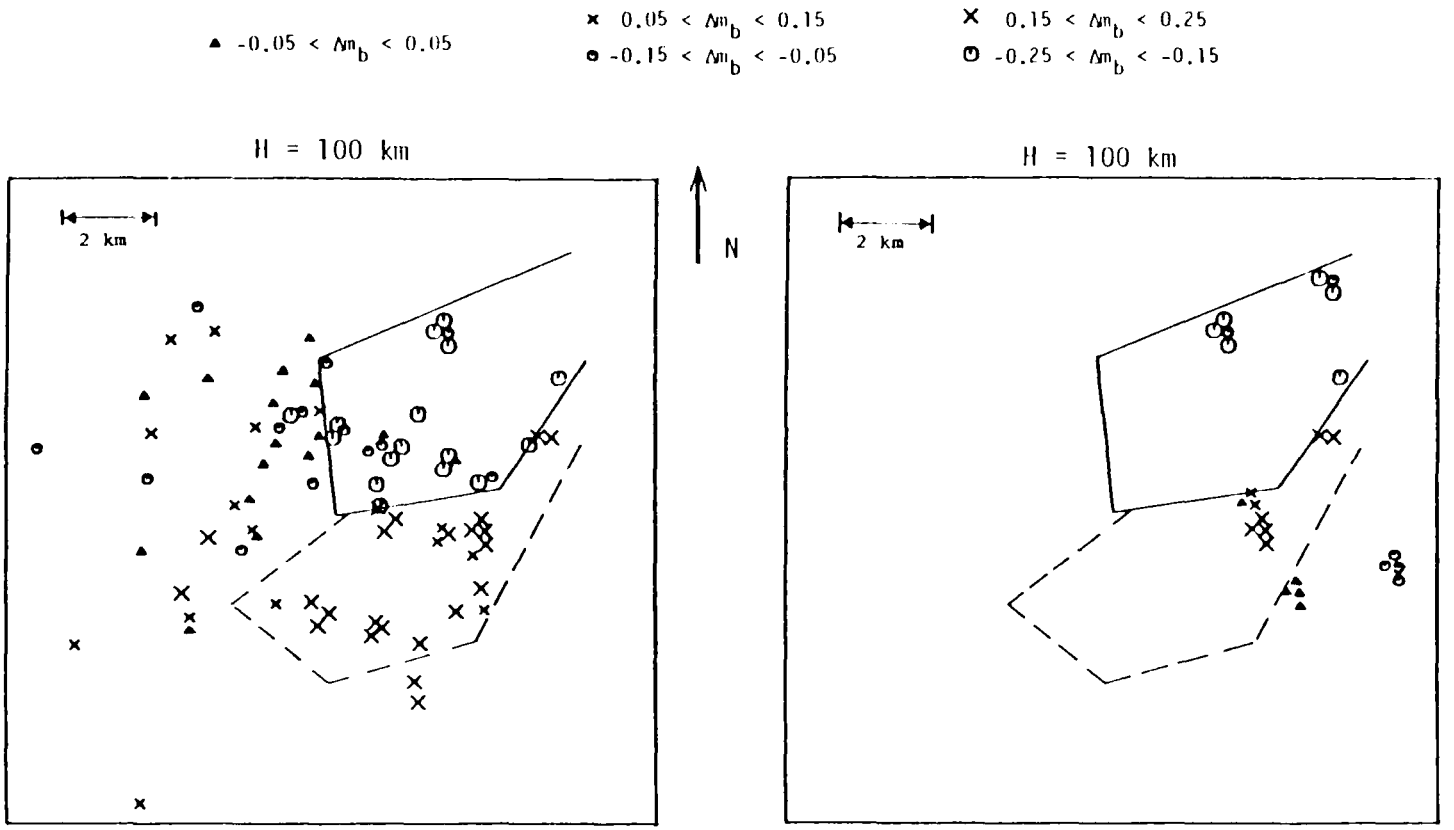

Figure 20. Four event residual pattern at a depth of 100 km, with boundaries of Figure 19 sketched in to show areas of predominantly large negative (solid line) and large positive (dashed line) residuals (left panel). Residuals from four stations in France selected to illustrate the consistent changes in the m_b residuals from normal to large positive to large negative (right panel).

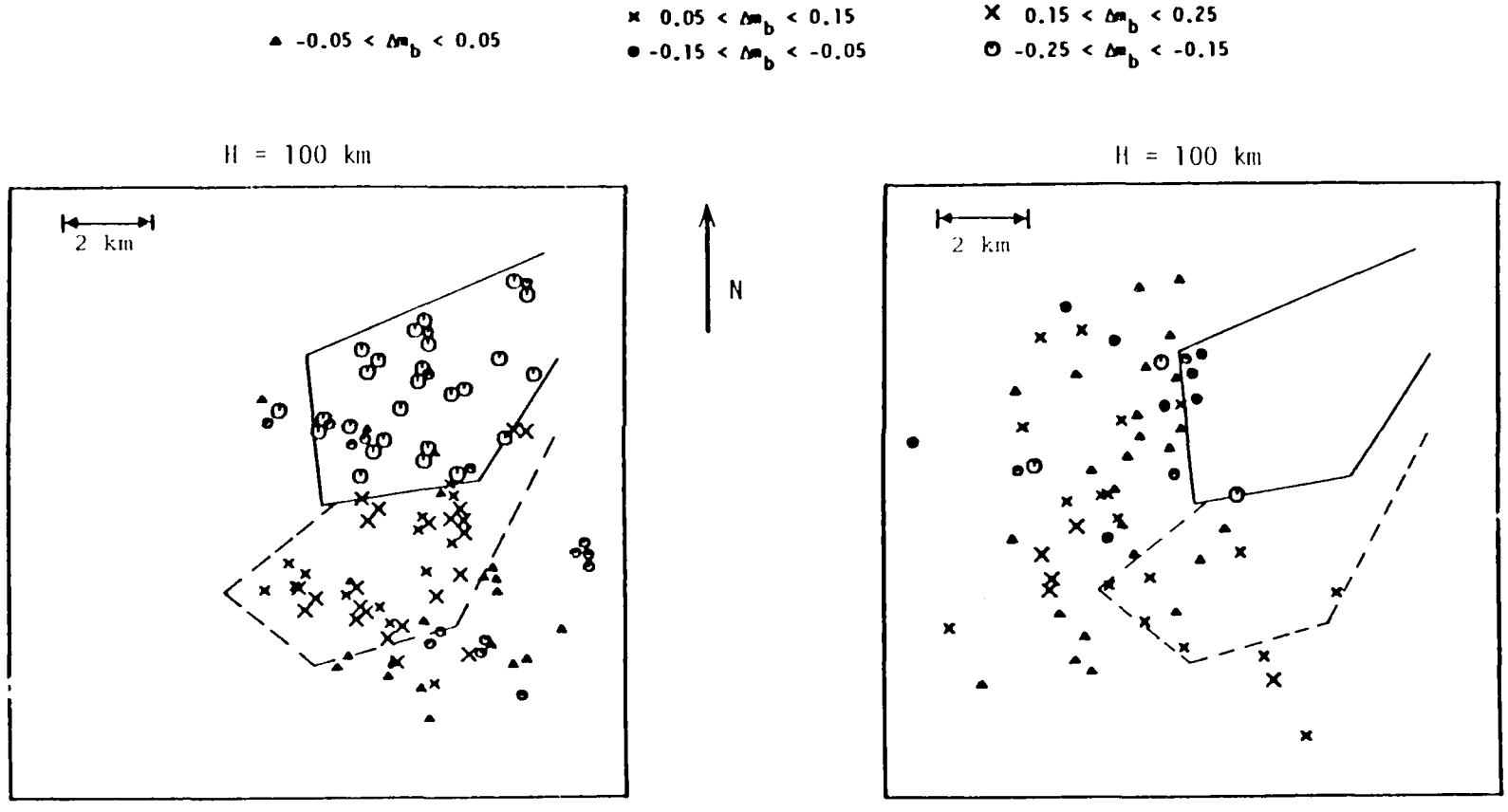

Figure 21. Nine event m_b residuals at a depth of 100 km, split into two groups of stations. The left panel contains those stations which contribute large negative residuals to the Northeast cluster of data, the right panel contains the remaining stations which project mainly outside the partitioned areas.

present a very consistent picture, with almost a complete separation of regions of low, normal and high residuals. In particular, the southern boundary of the large positive residual region seems to be well constrained by these data. The data from the remaining nine stations shown on the right hand panel project mainly outside the partitioned areas and represent a mix of mostly small positive and negative residuals. In fact, approximately 50 percent of these residuals are not significantly different from zero (i.e. solid triangles) indicating that the data from these stations are predominantly normal and, thus, presumably the P wave paths have not traversed the anomalous volume. These data serve to provide a rather tight constraint on the western boundary of the anomalous area.

Thus, our preliminary explanation for these observations is that the P wave paths to the stations characterized by large positive and negative m_b residuals have traversed an anomalous volume of material at a depth of about 100 km beneath the surface at a location northwest of the Shagan River test site (cf. Figure 11). The apparent dimension of the anomaly is on the order of 5 km and results in a defocusing of P wave energy out of the northern paths to the French stations (solid outline on Figure 21) and into the southern paths to the French stations (dashed outline). Presumably the anomalous volume corresponds to some sharp lateral variation in physical properties, in particular P wave velocity, at this 100 km depth. Available geologic maps indicate no surface expression of this anomaly, which is not surprising given its relatively great depth. The anomaly produces about 0.4 unit variation in the m_b residuals for these events. Cormier (1987) estimates that a 6-8 percent variation in velocity can cause amplitude variations of this order, although this must be considered a very rough estimate in that calculations in Cormier (1987) are not applicable to the scale size (i.e. wavelength/length) represented by our data.

It is important to note that m_b residual variations comparable to those documented above are also observed along other azimuths from the Shagan River testing area. For example, Figure 22 shows the station-corrected m_b residuals as a function of event location for the WWSSN

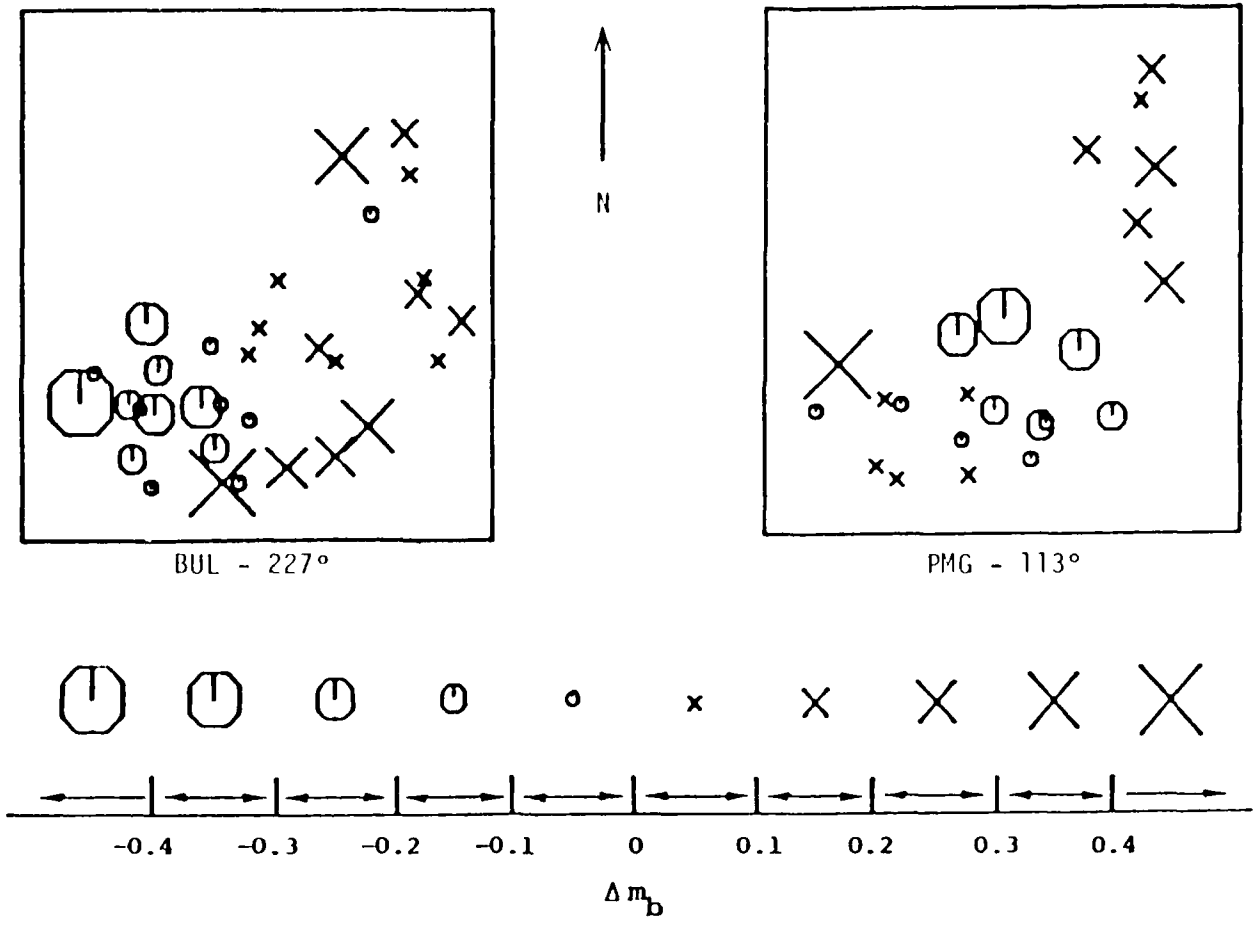

Figure 22. Station-corrected m_b residuals as a function of event location for WWSSN stations BUL in Africa and PMG in New Guinea, at the denoted recording azimuths.

stations BUL in Africa and PMG in New Guinea. It can be seen that these residuals also show pronounced trends, with residuals of the same sign tending to cluster into geographical groups. In the absence of denser coverage of the focal sphere in these azimuths, it is not possible to perform the kinds of detailed analyses that were previously performed using the m_b values observed at the European stations. However, these data suggest that the same m_b residual variations used to localize the anomalous structure along propagation paths from the Shagan River test area to Europe appear to occur along other propagation paths as well. Presumably, if adequate samples of single-station m_b data were available, the extent of other anomalous structures in the upper mantle/crustal regions surrounding Shagan could be determined in a similar manner.

III. ANALYSIS OF WAVEFORM DATA

3.1 INTRODUCTION

The analyses summarized in the preceding section confirmed the fact that the teleseismic m_b data provide strong evidence of systematic geophysical variations within the Shagan River testing area of the U.S.S.R. They were also used to illustrate how, in some cases, these data can be used to qualitatively map the subsurface structures responsible for this variability. In this section we explore other characteristics of the teleseismic data to determine whether they correlate with the observed m_b variations in a manner which provides additional insight into the nature of the near-source structural effects. In particular, we will attempt to determine whether single-station m_b residuals are correlated with variations in the spectral content or complexity of the waveforms from which the m_b values were measured. Changes in complexity could conceivably result from preferential focusing or defocusing of the direct P waves relative to P coda while changes in spectral content might result from preferential focusing/defocusing in certain narrow frequency bands. We will also investigate whether there is any evidence of travel time variations accompanying variations in m_b using the database compiled for this section. Since our prior results indicated that events in the central and northeastern sections of the test site show the most pronounced m_b variability with source location, the analyses will focus on a subset of events from those areas. The data analyzed consists of short-period P wave and P-coda recordings from the nine GDSN stations shown in Figure 23. These particular stations were selected on the basis of availability of digital waveform data with good signal-to-noise characteristics for a large proportion of the events of interest. Of the nine stations, GRFO and TOL lie near to the European stations used in Section II to locate the structural anomaly to the northwest of the test site. Thus, potential waveform variations at these stations are of special interest. The other seven stations are scattered throughout the remaining areas of the focal sphere, providing representative coverage for events located in the Shagan River test area.

Figure 23. Map locations of selected GDSN stations shown on an azimuthally equidistant projection centered on the Shagan River test site.

Since we are interested in waveform characteristics which might correlate with variations in single-station m_b residuals, single-station m_b values were first measured in the conventional manner from the maximum P wave amplitude of each waveform in the database. Next, single-station m_b residuals were computed for each station by subtracting the network m_b values for each event, and the resulting residuals were zero-meaned at each station by removing the average residual for all events measured at that station. As before, in the absence of any underlying deterministic mechanisms, it would be expected that the residuals for a given station would be randomly distributed with respect to event location. For some of these GDSN stations, however, this is not found to be the case. For example, Figures 24 and 25 show the station-corrected m_b residuals as a function of event location at stations TOL, GRFO, CHTO and BCAO (the remaining station plots can be found in Appendix A). As was observed for the stations analyzed in Section II, the residuals for some of these stations show trends such that residuals of the same sign tend to cluster into geographical groups, although the range of variations is generally smaller than those shown for the European stations in Section II. Perhaps the clearest and largest patterns of m_b variation associated with source location for these stations is at station TOL in Spain, which lies close to the stations in France which showed similarly large variations in the previous section. Moreover, comparison with Figure 6 indicates that the pattern of variation at station TOL is quite consistent with that observed previously at the French stations. On the other hand, station GRFO (Figure 24) in Germany shows a mixed pattern of variation, similar to those observed previously for the ISC stations in Germany. Thus, the data from these two stations are consistent with those observed from the nearby ISC stations used to identify the subsurface structural anomaly in Section II and, consequently, should provide a basis for more sophisticated signal analysis.

Regardless of the cause of the changes in m_b residuals with event location, one might expect a visual comparison of the signals recorded at a particular station to give some indication of anomalous behavior in cases where the m_b residuals vary by up to a few tenths of a

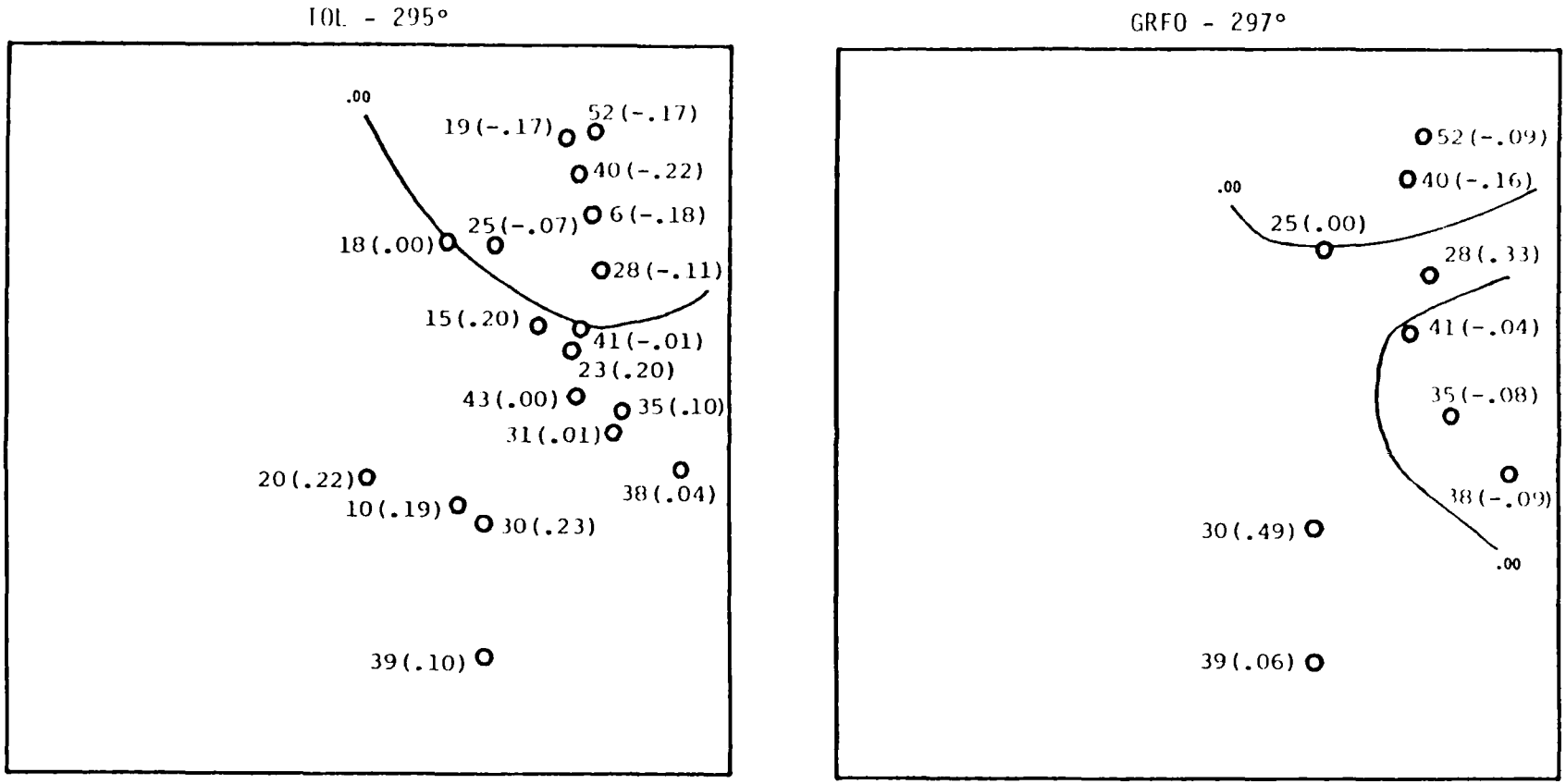

Figure 24. Station-corrected m_b residuals as a function of Shagan River event location for stations TOL and GRFO at the denoted recording azimuths.

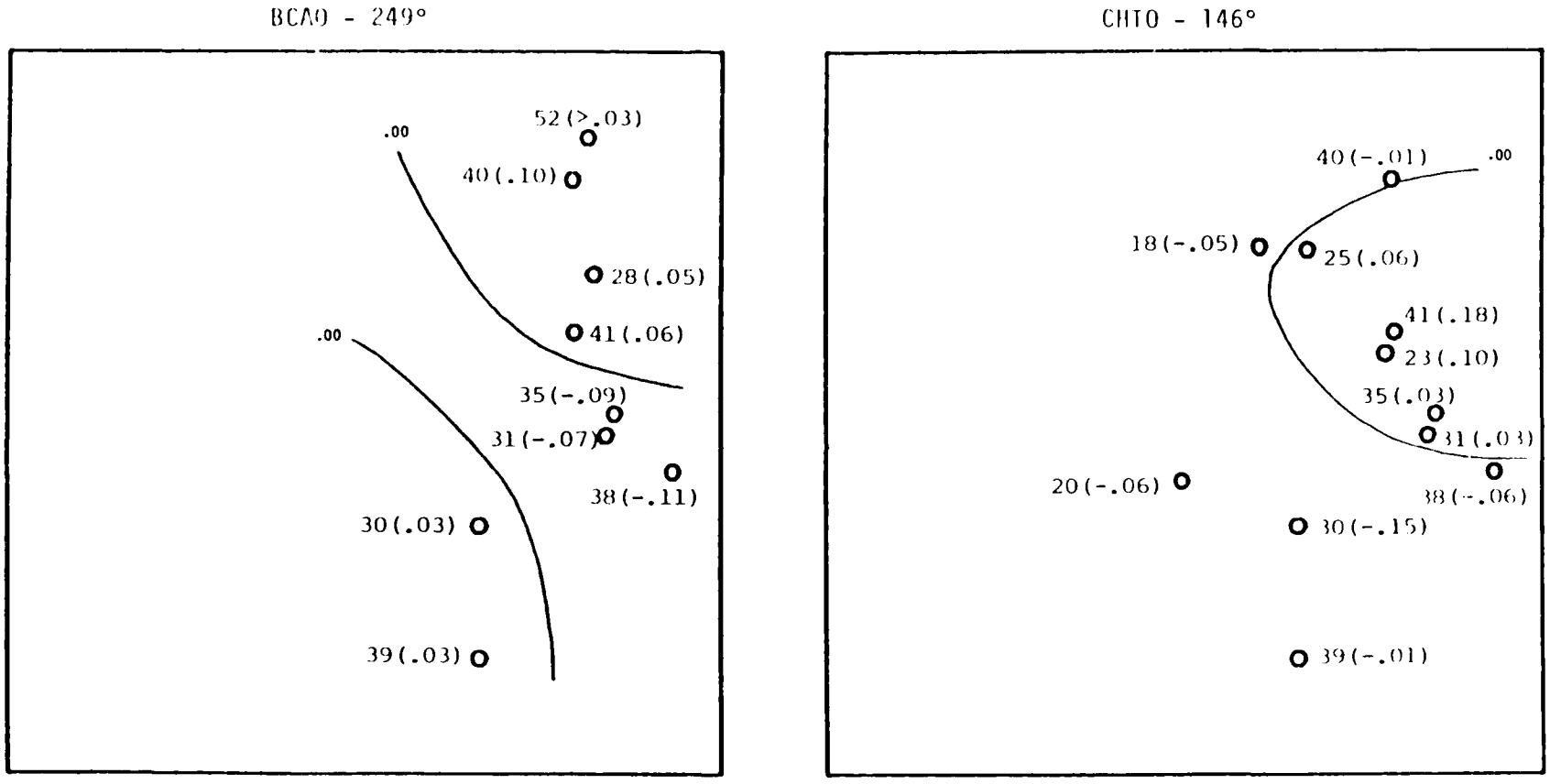

Figure 25. Station-corrected m_b residuals as a function of Shagan River event location for stations BCAO and CHTO at the denoted recording azimuths.

magnitude unit. Consequently, the recorded waveforms at stations TOL, GRFO, CHTO and BCAO are displayed in Figures 26 through 29, arranged in order of increasing m_b residual for each station. It is clear from these figures that a simple visual comparison of the P wave recordings gives no indication of any large, systematic differences which might be correlated with the m_b variation. Some signals do appear to have certain characteristics that make them appear different from others at the same station (e.g. event #28 at station GRFO), but there is no evidence of any consistent changes occurring as the m_b residuals go from negative to positive at any of the stations. In fact, it is quite surprising how similar the waveforms are at some stations (e.g. CHTO) in view of the variations in explosion size, source depth, and location. The waveforms recorded at the other five selected GDSN stations are reproduced in Appendix B where it can be seen that similar comments apply regarding the overall lack of correlation between general waveform characteristics and event m_b residual. Thus, a simple visual inspection of the signals for this group of stations reveals no easily identifiable features which might be associated with anomalous m_b behavior.

3.2 COMPLEXITY RESULTS

In order to better quantify any subtle changes in complexity which might be taking place, we have computed the temporal centroid of each time history over a 20-second P wave and P-coda window, defined as (Lay and Welc, 1987)

$$C = \frac{\sum_{i=1}^{N} \left(x_i^2 \cdot \frac{i}{sr} \right)}{\sum_{i=1}^{N} x_i^2}$$

where

N = number of points

sr = sampling rate

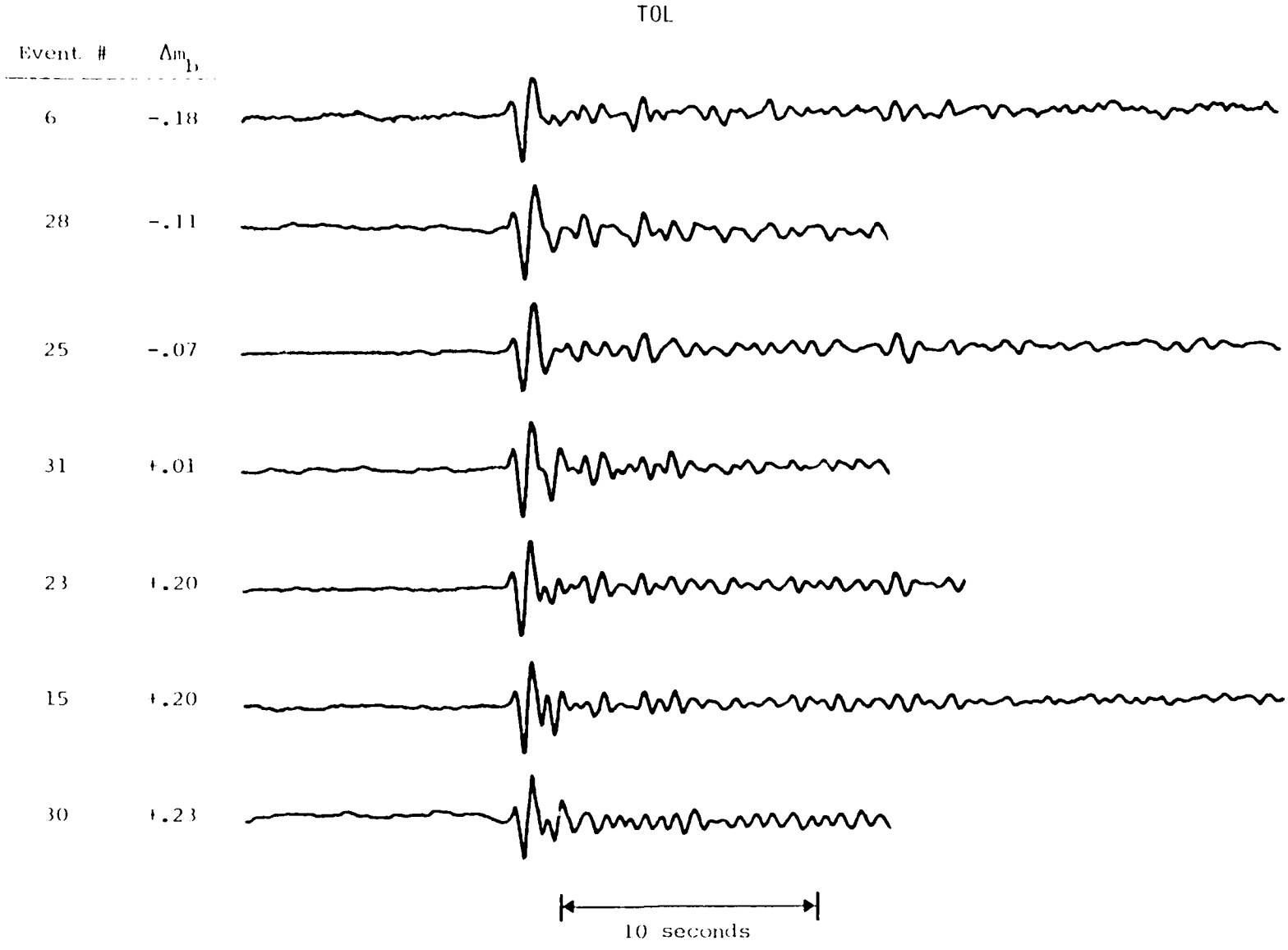

Figure 26. Teleseismic short-period P waveforms recorded at station TOL from Shagan River explosions, in order of station m_b residual.

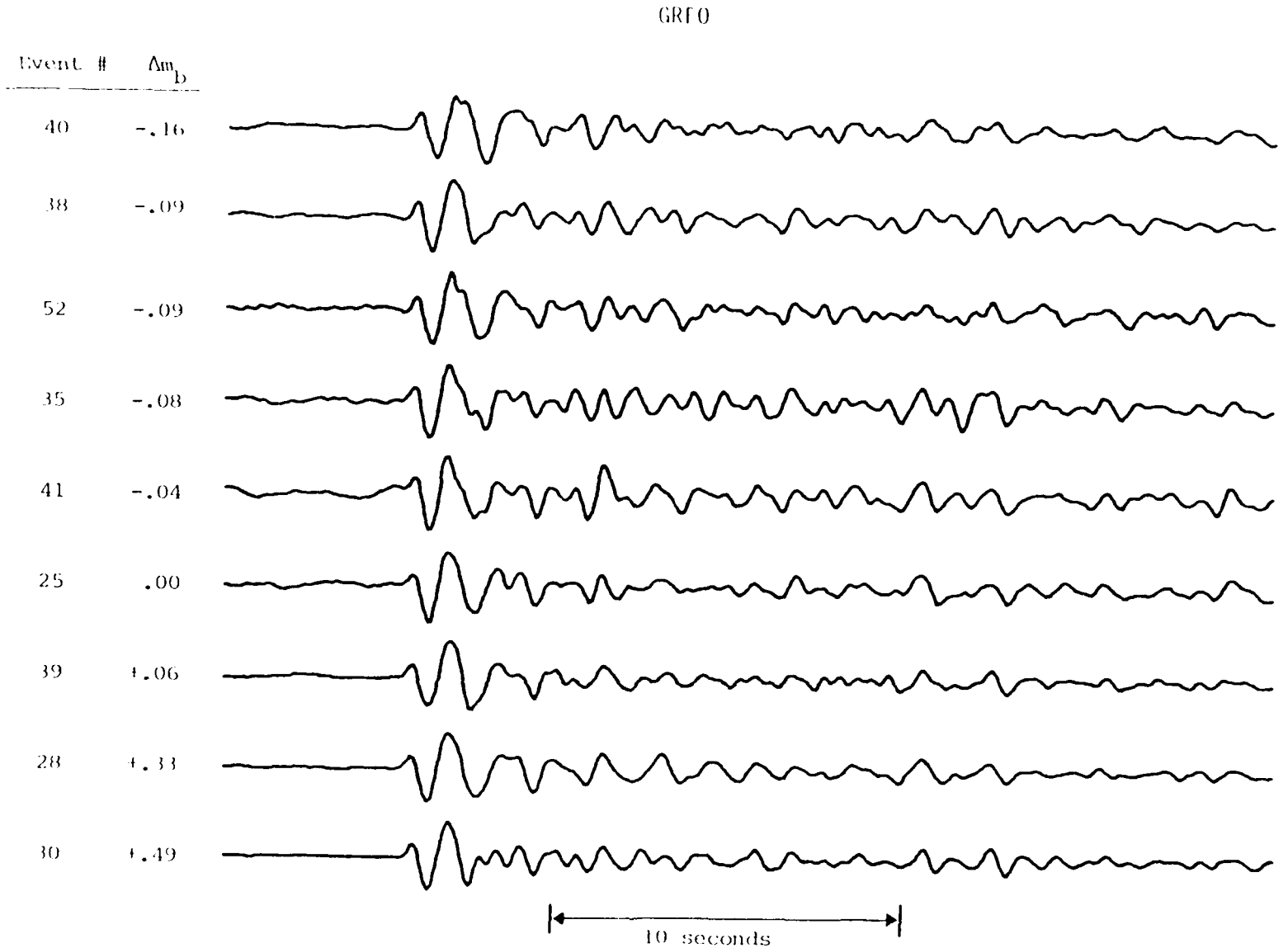

Figure 27. Teleseismic short-period P waveforms recorded at station GRFO from Shagan River explosions, in order of station m_b residual.

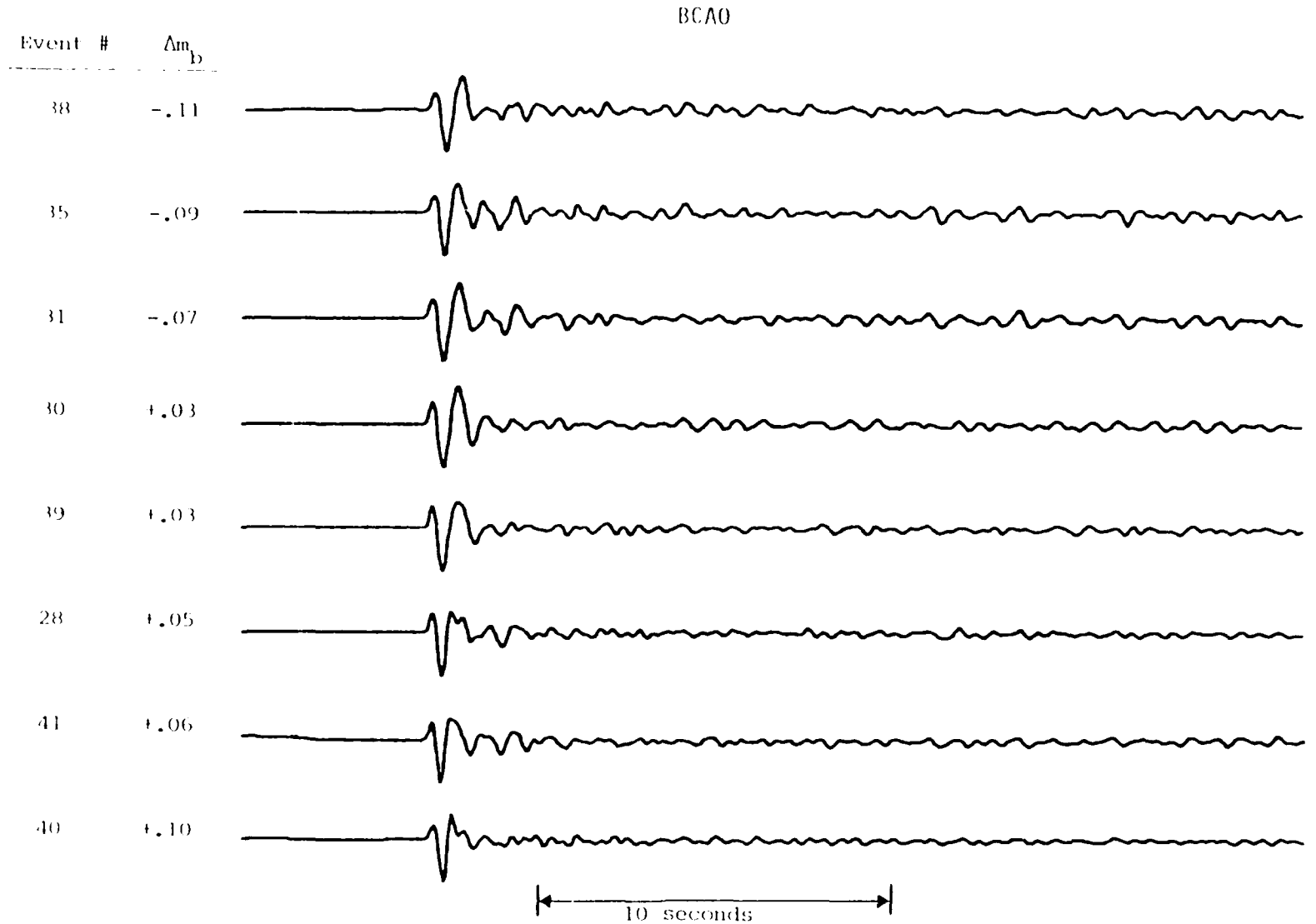

Figure 28. Teleseismic short-period P waveforms recorded at station BCAO from Shagan River explosions, in order of station m_b residual.

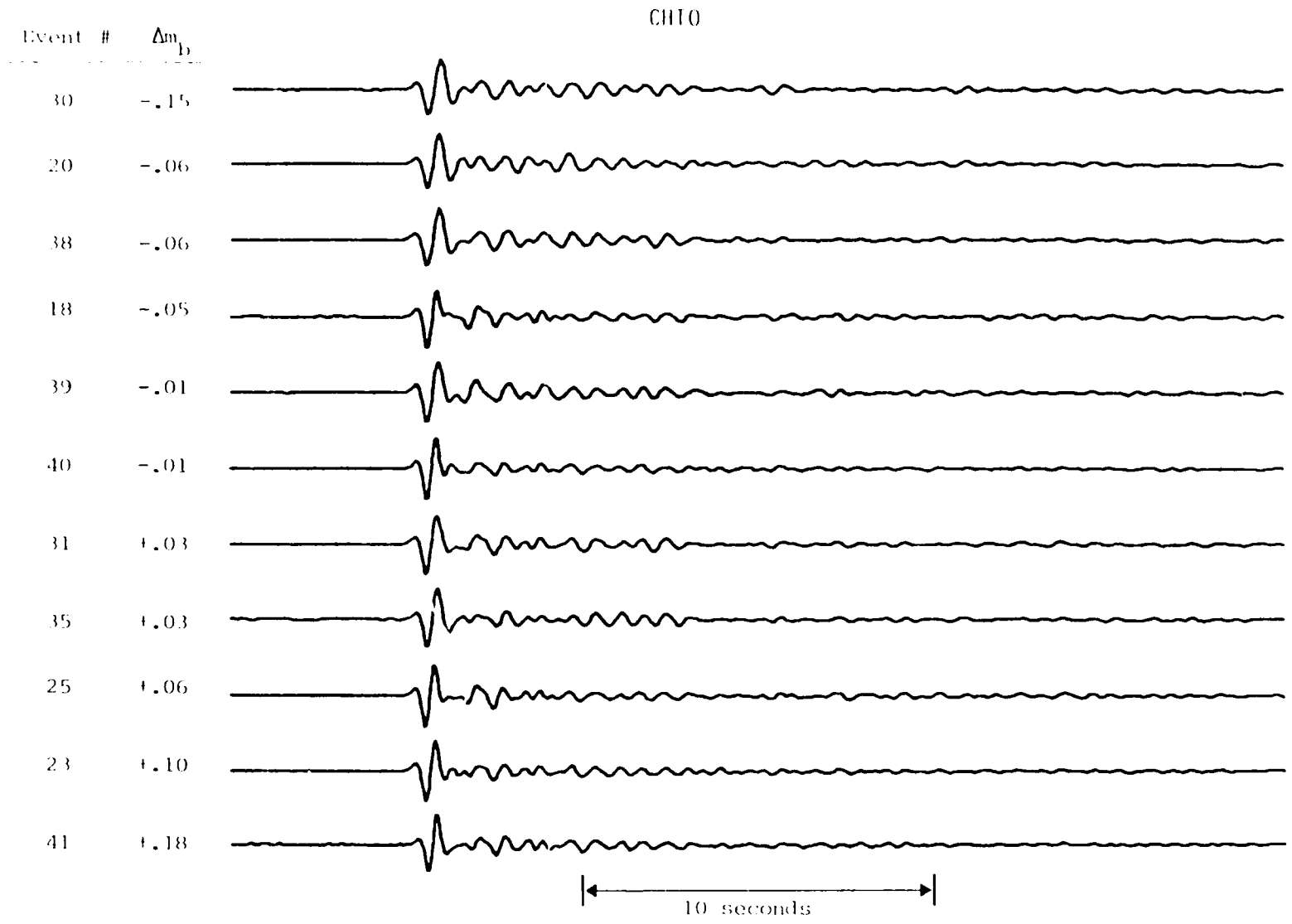

Figure 29. Teleseismic short-period P waveforms recorded at station CHIO from Shagan River explosions, in order of station m_b residual.

Thus, larger values of the temporal centroid indicate relatively larger P-coda amplitude/P amplitude (i.e. greater complexity) and vice versa. A station-by-station comparison of the temporal centroids vs. the m_b residuals reveals two general categories of stations. The first group consists of those stations with large scatter and with no indication of a trend in centroid values as the m_b residuals change from negative to positive. The other group of stations consists of those also having large scatter but with some hint of a trend toward decreasing centroid value (i.e. decreasing complexity) as the m_b residuals increase. The results for this latter group, which includes stations TOL and GRFO, are shown in Figure 30. It can be seen here that for these six stations there appears to be a slight correlation between decreasing complexity and increasing m_b residual, with some stations showing this pattern more clearly than others. As an illustration of this correlation, Figure 31 shows a comparison of waveforms at station TOL from event #28, which has a residual of -.11 magnitude units and a relatively large centroid value (marked as C_i on the plot), and event #23 which has an m_b residual of +.20 and a slightly smaller centroid value. This figure shows that while there do appear to be quantifiable differences in complexity between events with large and small m_b residuals at a given station, these variations are not easily resolved by the naked eye. Figure 32 shows some other waveform comparisons for station BCAO. In this case the differences between the events with large and small centroid values, while subtle, are visually more noticeable. Finally, Figure 33 shows a similar comparison between events #35 and #39 at station GRFO, where the changes in complexity are more obvious. Thus, at some stations there appear to be quantifiable differences in complexity between events showing large m_b residual differences. For most stations, however, these changes are either not present or are too small to be detected using this processing technique.

3.3 SPECTRAL RESULTS

In an attempt to quantify any spectral variations which might be associated with variations in m_b residuals all the GDSN waveforms were

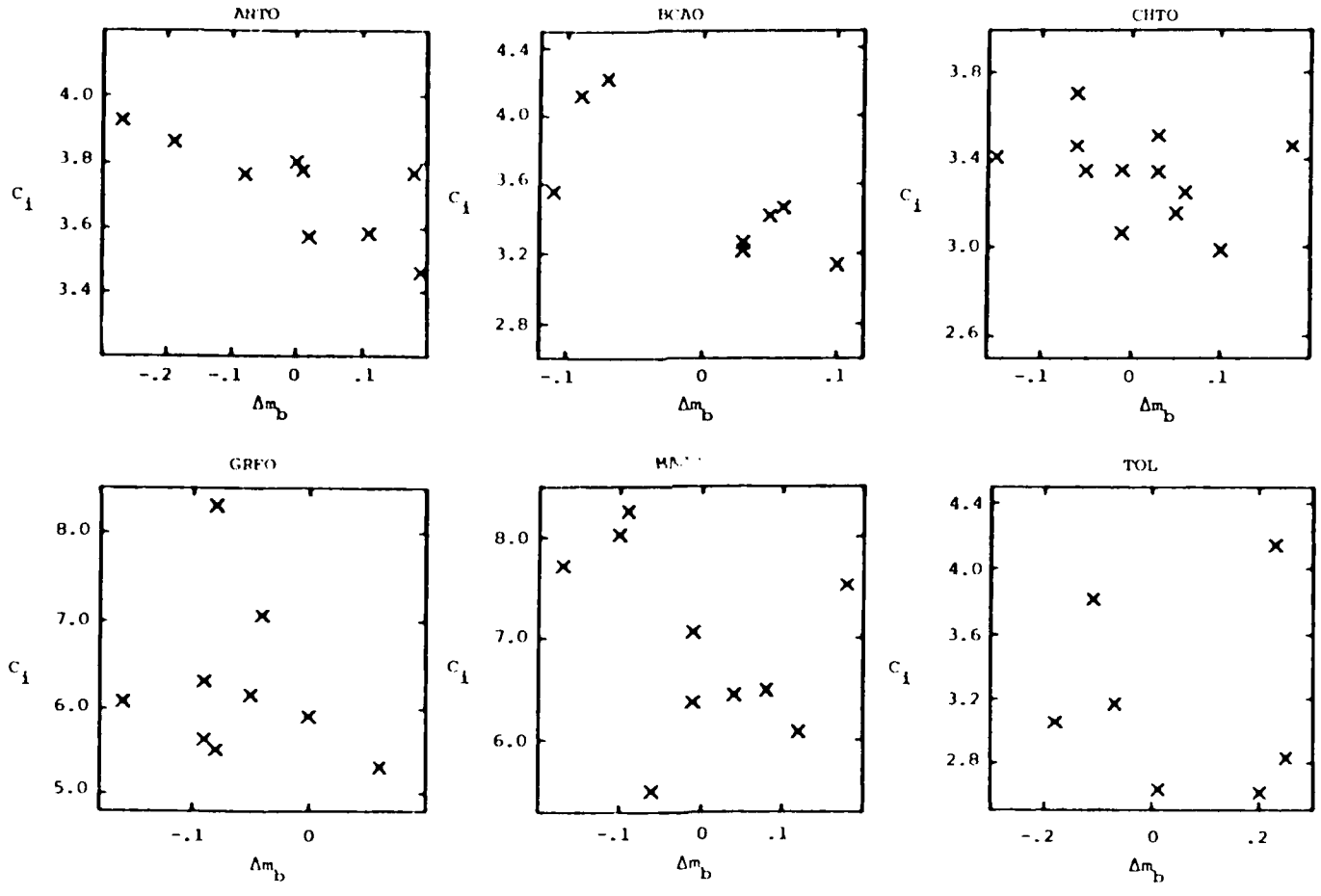

Figure 30. Temporal centroid values (C_i) versus m_b residuals at stations ANTO, BCAO, CHTO, GRFO, MAJO and TOL.

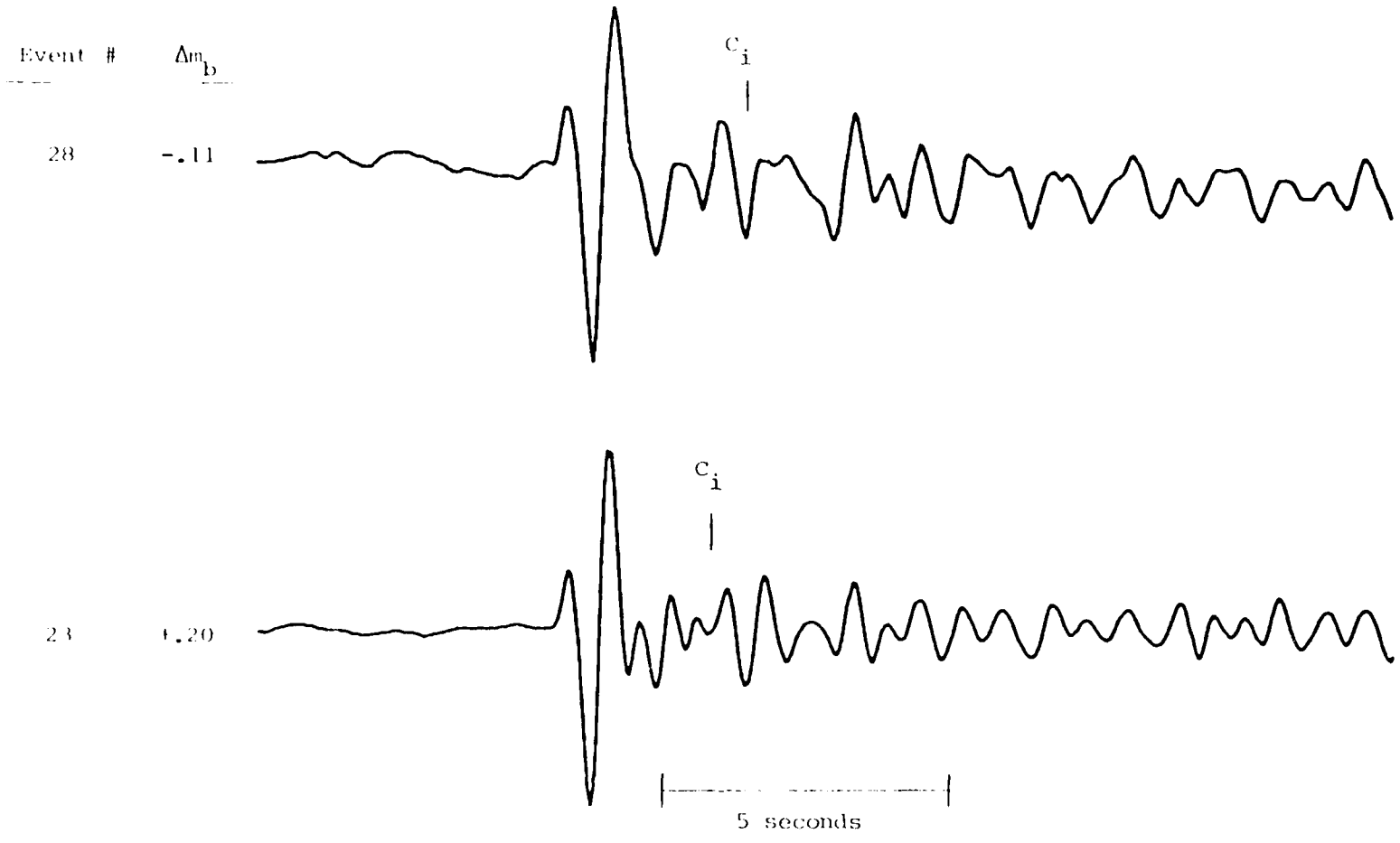

Figure 31. Comparison of waveforms from events #28 and #23 with different centroid values (C_i) at station TOL.

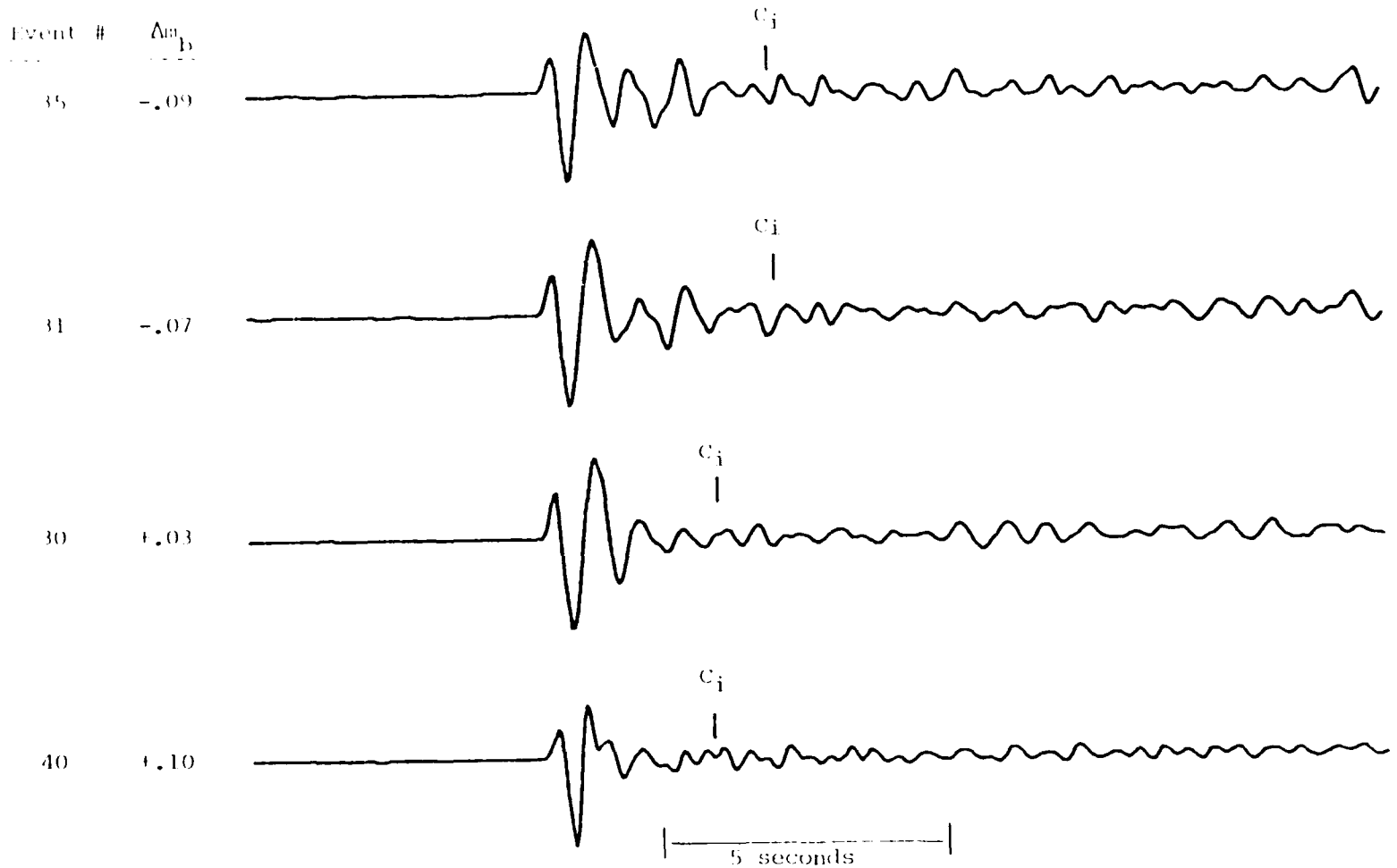

Figure 32. Comparison of waveforms from events #35, #31, #30 and #40 with different centroid values (C_i) at station BCAO.

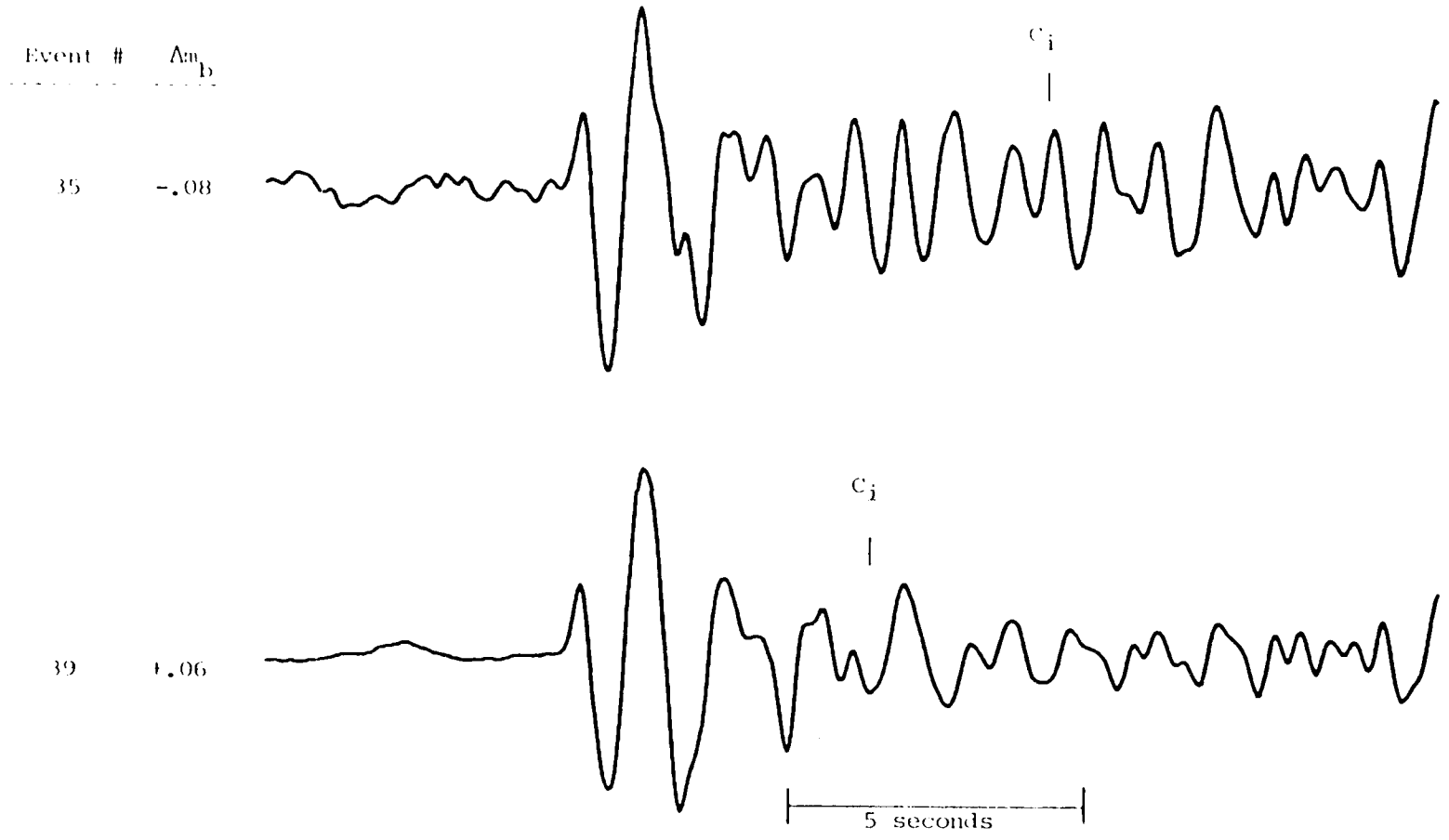

Figure 33. Comparison of waveforms from events #35 and #39 with different centroid values (C_i) at station GRFO.

bandpass filtered into six separate frequency bands with center frequencies ranging from 0.6 Hz to 3.8 Hz. After testing for adequate signal-to-noise characteristics, spectral ratios were computed for each waveform by dividing the filtered trace maximum amplitudes from each of the four high-frequency bands by those for the two low-frequency bands. Thus, changes in the spectral ratios at a given station provide a measure of the variation in spectral shape from event-to-event. At each station, the individual spectral ratios were then examinec for any correlation with the m_b residuals as measured from the same waveforms. As with the complexity measurement, a number of stations showed no correlation between any of the spectral ratios and the m_b residuals. For these stations, the near-source effect which is causing m_b residuals to vary by up to a few tenths of a magnitude unit is apparently a broadband effect. Some stations, however, did show trends when particular spectral ratios were correlated with the m_b residuals. This is illustrated more clearly in Figure 34, which shows how spectral ratio variations correlate with m_b residual variations at stations TOL, ANTO, BCAO and CHTO. For these stations the variations in spectral content are such that a positive m_b residual is associated with enhanced high-frequency energy, or vice versa. Now, a confounding factor in these spectral comparisons is the fact that the event magnitudes vary. In order to minimize spectral variations which might be due to changes in the event magnitudes, direct comparisons were also made between bandpass output amplitudes for groups of events of approximately the same network magnitude. Figure 35 shows a comparison of bandpass spectra for two pairs of events having spectral variations which correlate with m_b residual variation as recorded by station TOL. In this and subsequent figures of the same type, the spectra have been normalized to a constant value at 1 Hz. It can be seen that for these pairs of events of comparable magnitudes the enhancement of energy at frequencies above 1 Hz relative to energy at or below 1 Hz is associated with a positive shift in the m_b residuals. Similar event comparisons are shown for stations ANTO, BCAO and CHTO in Figure 36. Once again, the enhancement of energy above 1 Hz relative to energy at or below 1 Hz is associated with positive m_b residuals. An interpretation of these

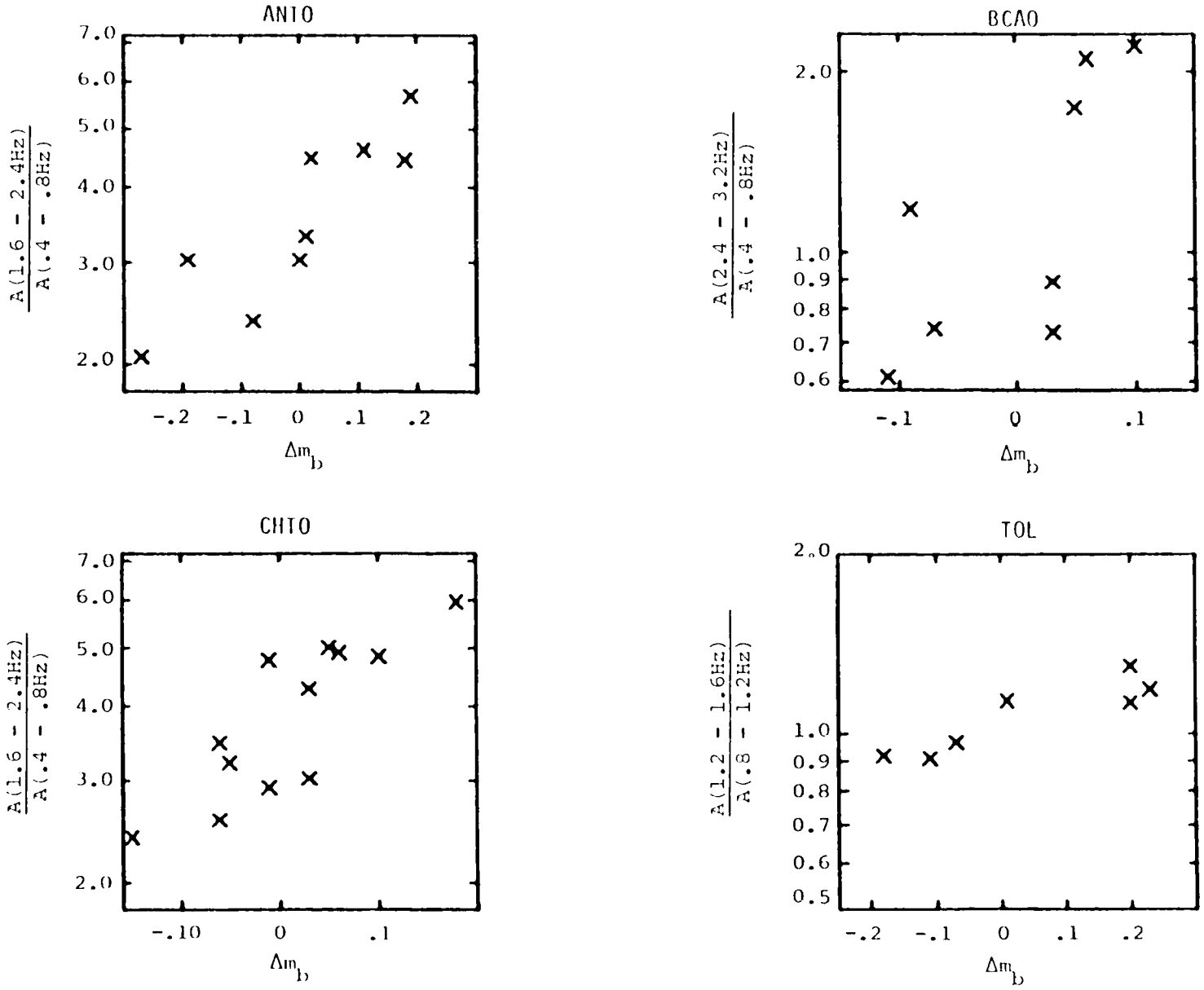

Figure 34. Spectral ratio values versus m_b residuals at stations TOL, ANTO, BCAO and CHTO.

Event #	Event m_b	Δm_b
15	5.74	+.25
25	5.59	-.07

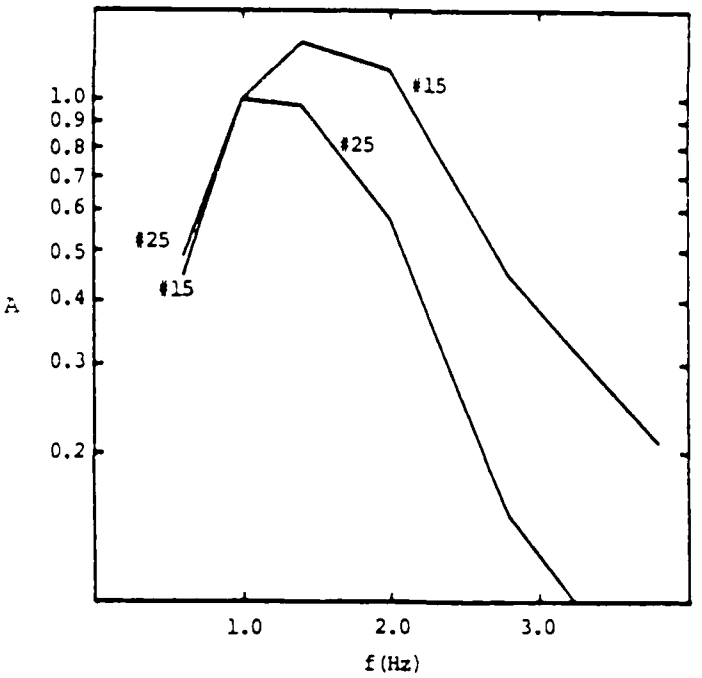

Event #	Event m_b	Δm_b
23	5.93	+.20
28	5.86	-.11

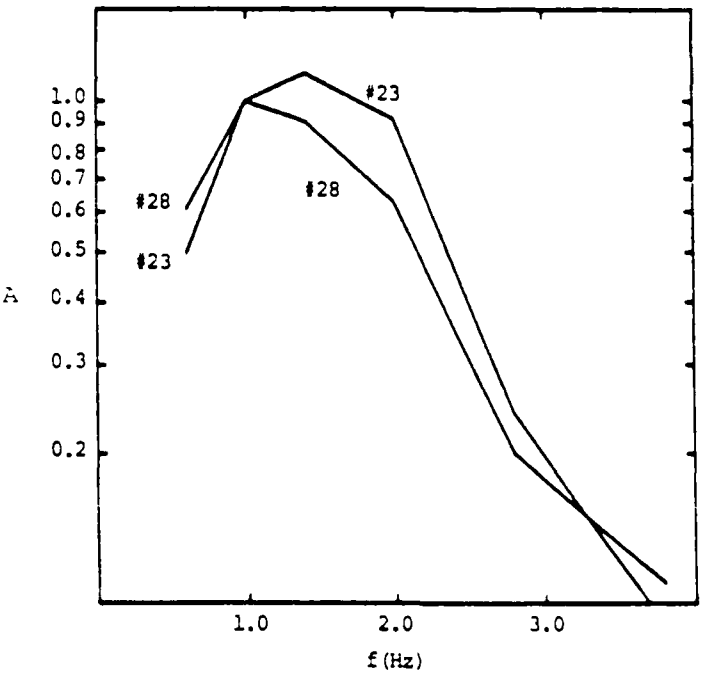

Figure 35. Spectral comparisons of selected Shagan River explosions at station TOL.

ANTO

Event #	Event m_b	Δm_b
28	5.86	+.11
38	5.84	-.19
40	5.93	-.27

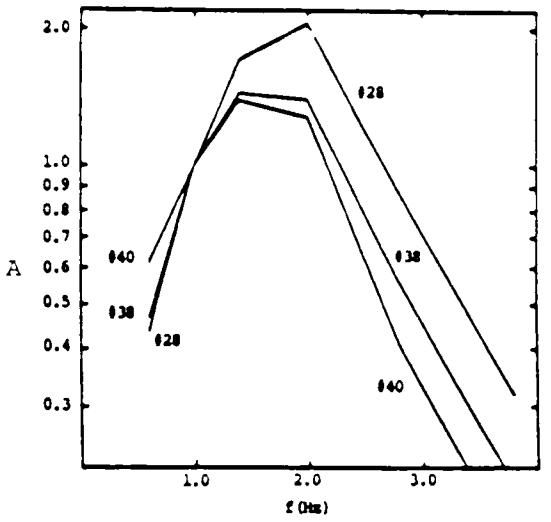

BCAO

Event #	Event m_b	Δm_b
40	5.93	+.10
28	5.86	+.05
31	5.98	-.07
38	5.84	-.11

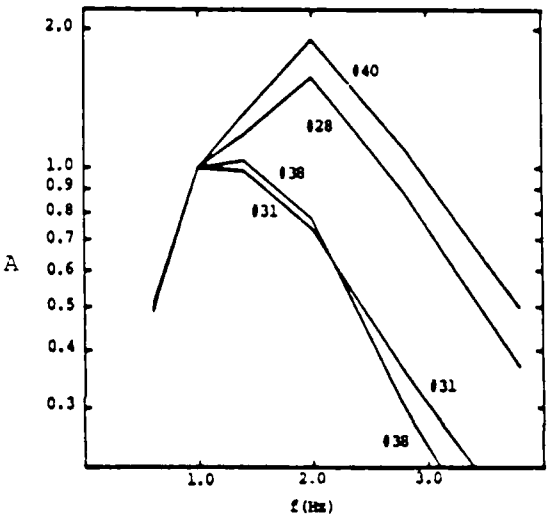

CHTO

Event #	Event m_b	Δm_b
23	5.93	+.10
38	5.84	-.06

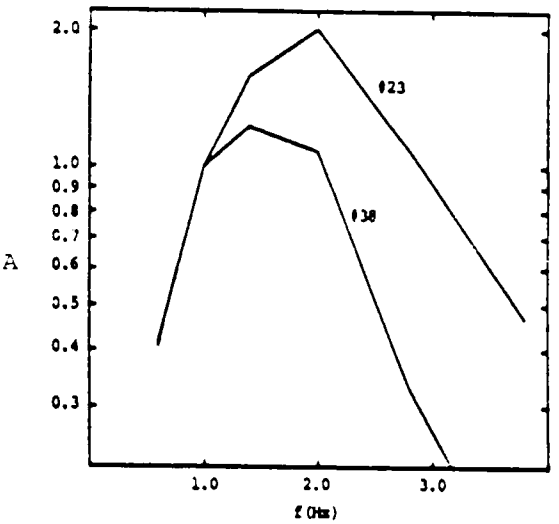

Figure 36. Spectral comparisons of selected Shagan River explosions at stations ANTO, BCAO and CHTO.

results is that high-frequency energy is being preferentially focused/defocused at or near the source. This is supported by the fact that the network magnitudes for the events that are being compared are similar and the travel paths from the events to any single station are essentially identical except for the portion nearest the source. One station which shows a slight correlation of the opposite sense from the above, that is, positive m_b residuals associated with depleted high frequency energy, is station GRFO in Germany. While not very pronounced, this correlation is noteworthy in that it is the only one of it's kind among this group of stations. This effect is illustrated in Figure 37 which shows a comparison of filtered time series for events with large positive and negative residuals at station GRFO. In this figure the trace amplitudes of the two higher frequency traces are scaled to the amplitude of the low frequency trace for each event separately, and it can be seen that event #28, with a positive m_b residual, has relatively less high frequency energy than event #41 with a negative residual.

In summary, about half of the stations analyzed show no distinguishing variations in P wave spectral characteristics which can be associated with m_b residual variations. However, some stations, including station TOL in Spain, show some correlation between enhanced high-frequency energy and positive m_b residuals. This result suggests that additional digital waveform data from station TOL, or more specifically from stations in France, if they were available, might be useful in providing additional constraints on the characteristics of the structural anomaly found in Section II. That is, such data could be used to provide frequency dependent constraints on the sophisticated three-dimensional seismic modeling which will be required to uniquely invert for the characteristics of the subsurface structure producing the observed m_b anomalies.

3.4 TRAVEL TIME RESULTS

In Dermengian et al. (1985), it was concluded that the arrival time data reported to the ISC are not precise enough to resolve the rather small travel-time variations which might be expected to accompany

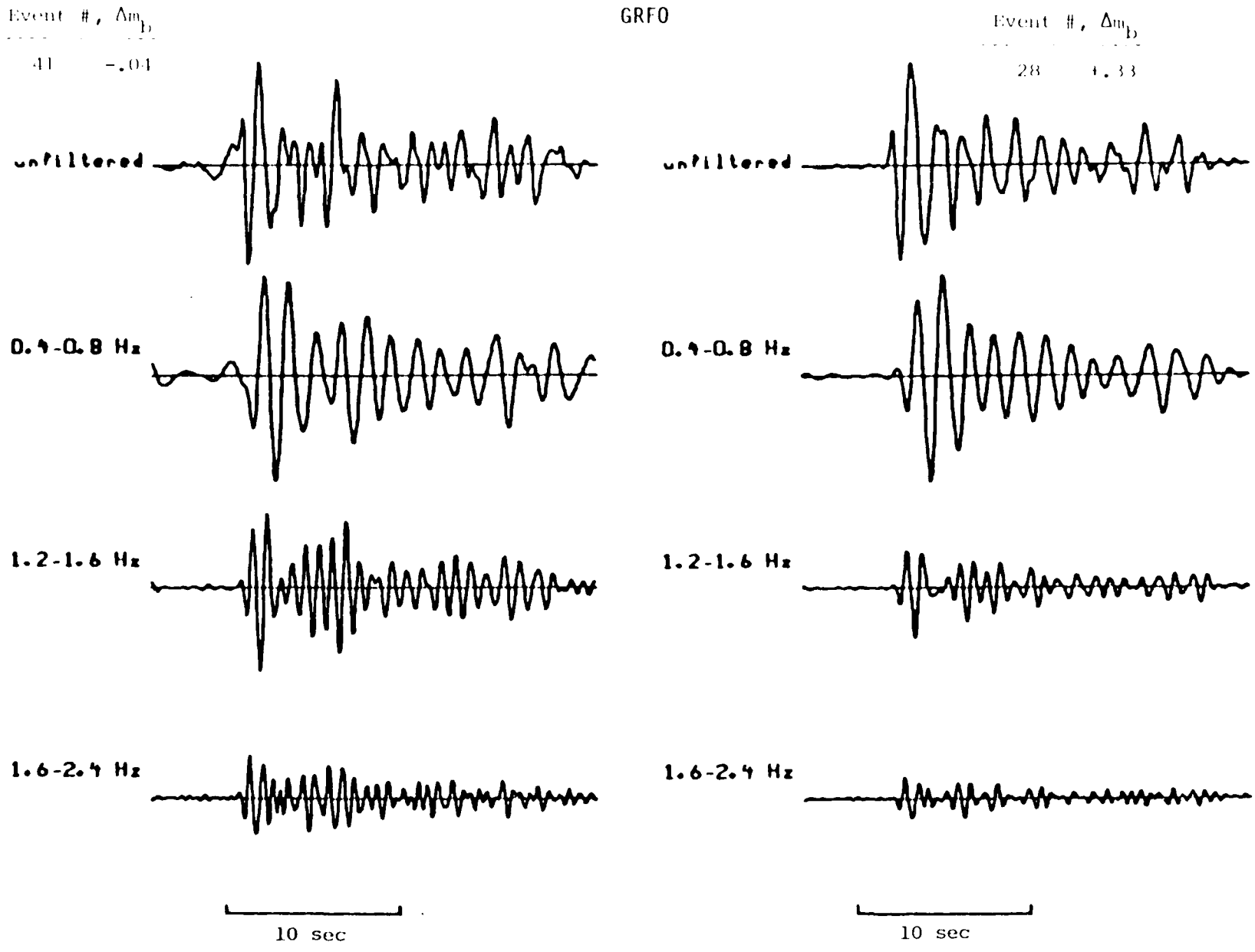

Figure 37. Comparison of filtered waveforms from selected Shagan River explosions at station GRFO.

the observed m_b variations. However, the GDSN recordings provide a more precise data base for testing for correlations between m_b and arrival time variations. Five stations were selected based on the results of Sections 3.2 and 3.3 (stations TOL, ANTO, BCAO, CHTO and GRFO) and arrival times were carefully measured to a precision of better than 0.1 seconds on all waveforms recorded at those stations from the events of interest. Travel time residuals were then computed by subtracting the travel times predicted by the Herrin P wave travel-time curves (Herrin et al., 1968) from the observed travel times. Then, by analogy with the m_b analysis described above, the mean travel-time residual was determined for each station, and subtracted from the individual observed residuals at that station to obtain the variation of the residuals as a function of source location. Upon inspection, these travel-time residuals were found to be quite small and to show no obvious correlation with event location at any of the stations. In an attempt to quantitatively determine whether the variation in the travel-time residuals was correlated in any way with the variation in the m_b residuals, the correlation coefficients between the two sets of residuals were estimated at each of the five stations. Of the five stations, two (BCAO and CHTO) showed nearly zero correlation between the two variables, while the other three (TOL, ANTO, GRFO) showed some positive correlation of late arrivals with positive m_b residuals. Figure 38 shows the relationship between the travel-time residuals and the m_b residuals at these three stations. It can be seen in this figure that the range in travel-time residuals is very small and the scatter large, but that there is some trend of late arrivals correlating with positive m_b residuals, particularly at station ANTO. The direction of this trend favors a focusing type mechanism as the cause of the m_b variations as opposed to an absorption or attenuation type mechanism which would generally cause late arrivals to be associated with negative m_b residuals. Clearly, it would be of interest to pursue such investigations further using more precise arrival time data from the French stations used to define the subsurface structural anomaly in Section II. Unfortunately, such data are not currently available.

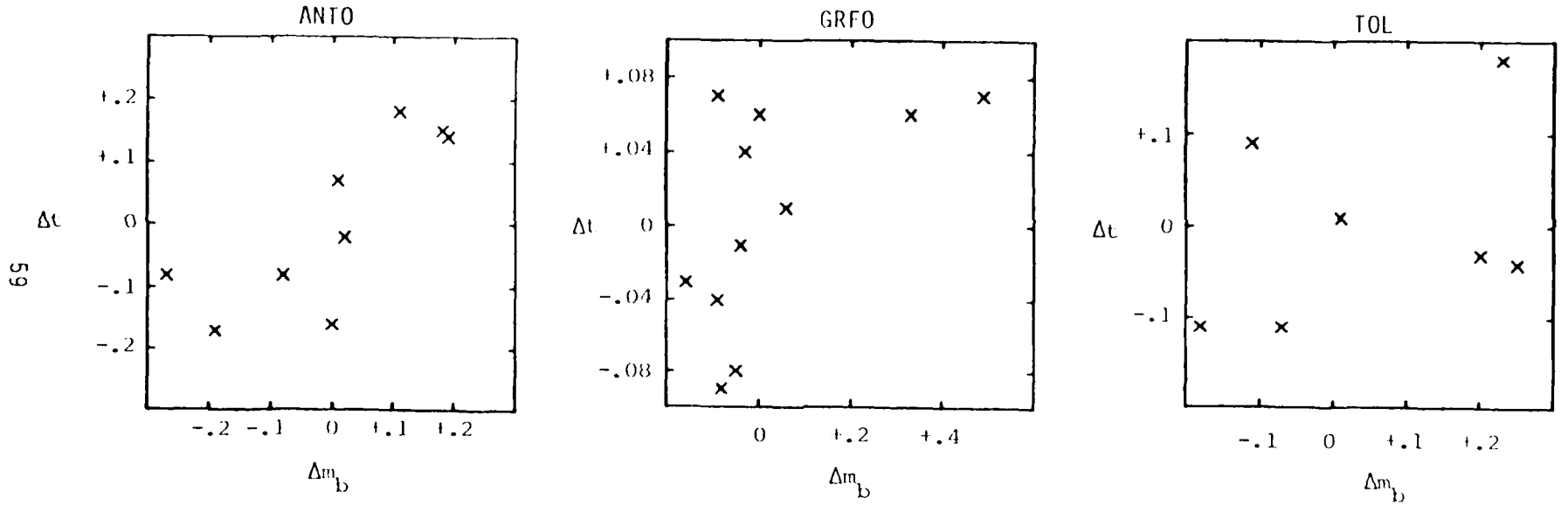

Figure 38. Travel-time residuals versus m_b residuals from Shagan River explosions at stations ANTO, GRFO and TOL.

IV. SUMMARY AND CONCLUSIONS

4.1 SUMMARY

The investigations summarized in this report have centered on an analysis of variations in P wave propagation characteristics along teleseismic paths from underground explosions conducted at the Shagan River test site. One of the key assumptions involved in the estimation of explosion yield from teleseismic P wave data is that variations due to propagation path effects can be averaged out if a suitably large, well-distributed network of observation stations is used. That is, it is assumed that, aside from possible source region effects which would be common to all teleseismic P-wave observations (e.g. those due to upper mantle Q variations beneath the test site) large network estimates of m_b are unbiased. Experience has confirmed that this assumption is generally valid, at least in a gross statistical sense. However, if one examines the data in any detail, it soon becomes evident that there is much about m_b variability which is still poorly understood. The primary objective of the present study has been to attempt to develop a better quantitative understanding of some of the sources of such m_b variability observed for explosions at the Shagan River test site.

The preliminary investigations of Dermengian et al. (1985) were reviewed in Section II, with particular emphasis on the nature of the observed m_b anomalies which were used to infer the existence of systematic geophysical variations within the Shagan River test area. The problem of network bias in the determination of average event m_b values was also addressed in this section, where the results of a correlation analysis performed on a large sample of single station m_b readings were used to obtain unbiased estimates of the m_b values associated with the explosions at this test site. These revised network-averaged m_b values were then used as references to quantitatively define the ranges in distance and azimuth over which the single station m_b anomalies persist. Once this was accomplished, a first order ray trace analysis was conducted in which the m_b residuals observed from a group of stations in Europe were projected onto planar surfaces at different depths using the known

azimuths and ray parameters for those stations. The results of this analysis indicated that the teleseismic P wave paths to stations in France from explosions located in a particular area in the northeast portion of the test site traversed an anomalous volume of material at a depth of about 100 km beneath the surface at a location northwest of the Shagan River test site. The apparent dimension of the anomaly is inferred to be on the order of 5 km and results in a defocusing of P wave energy out of the northern paths to the French stations and into the southern paths to the French stations. Presumably, the anomalous volume corresponds to some sharp lateral variation in physical properties, in particular P wave velocity, at this 100 km depth. A preliminary review of available geologic data revealed no surface expression of this anomaly at depth.

In Section III, a preliminary analysis of waveform data from a subset of the explosions was conducted in an attempt to define any near source structural contributions to the waveform time- and frequency-domain characteristics. That is, a database of teleseismic P wave recordings from a group of well-distributed stations was carefully analyzed in an attempt to identify any correlations between waveform characteristics and m_b residuals as determined from the same waveforms. A simple visual inspection of the signals revealed no obvious characteristics which could be associated with m_b residual variations of up to a few tenths magnitude unit. Further quantitative studies, however, showed that, in some cases, a correlation could be found between certain spectral and coda characteristics and m_b residuals. In particular, enhanced high-frequency energy appears to be associated with positive m_b residuals and relatively large complexity values appear to be associated with negative m_b residuals. Furthermore, in some cases an association can be found between delayed arrival times and positive m_b residuals. While these waveform analysis results are preliminary, they do suggest that the same near source phenomena responsible for the large variations observed in m_b residual behavior may also be influencing other measurable waveform parameters.

4.2 CONCLUSIONS

The analyses summarized above support the following principal conclusions regarding the nature of P wave propagation variation out of the Shagan River test site.

(1) Teleseismic m_b data provide strong evidence of systematic geophysical variations within the Shagan River testing area. In particular, there are large (0.5 m_b units) variations in the station-corrected m_b residuals with azimuth between explosions in close proximity in the northeast and central portions of the test site.

(2) The observed azimuthal variability in the m_b station corrections with source location indicates that the network-averaged m_b values for explosions at Shagan River will be dependent on the specific azimuthal distribution of the stations used to compute the averages. This dependence can be minimized by accounting for station-station correlations in the network averaging procedure.

(3) Variations in m_b residuals for stations in a given azimuth and distance range which have positive station-station correlation are systematic enough that they can be contoured as a function of source location. The resulting contours reveal that the largest m_b variations take place along propagation paths from the Shagan area to seismic stations in France, with lesser variations occurring along paths to other European stations and to North American stations.

(4) When the teleseismic m_b residuals from seismic stations in continental Europe are projected back into the corresponding P wave initiation areas near the source they reveal

the existence of an anomalous volume of material located northwest of the test site at a depth of about 100 km. This anomalous volume apparently defocuses energy out of certain ray paths and redirects the energy into other ray paths. Presumably this anomalous volume corresponds to some sharp lateral variation in physical properties, in particular P wave velocity, at this depth. Available geologic maps indicate no surface expression of this anomaly.

(5) Teleseismic m_b data from WWSSN stations to the south and southeast of the test site reveal that propagation anomalies also occur along these azimuths. However, the distribution of observing stations in these azimuths is not dense enough to permit the corresponding structural anomalies to be isolated using the kinds of detailed analysis procedures which were applied to the European data.

(6) In some cases, the observed patterns of m_b residual variations can be correlated with similar patterns of variation in either spectral composition, coda complexity or arrival times of the P wave signals. The sense of these variations is such that enhanced high frequency energy, decreased coda complexity and delayed arrival times are all associated with a positive shift in the m_b residuals. Unfortunately, these correlations are generally not very well defined and waveform data are not currently available from the French stations showing the most pronounced m_b variability. Analyses of such data could provide much insight into the relationship between m_b and waveform variability.

REFERENCES

Barker, B. W. and J. R. Murphy (1986), "An Analysis of the Effects of Tectonic Release on Short-Period P Waves Observed From Shagan River Explosions," SSS-R-87-8422, December.

Cormier, V. F. (1987), "Focusing and Defocusing of Teleseismic P Waves By Known Three-Dimensional Structure Beneath Pahute Mesa, Nevada Test Site," Bull. Seism. Soc. Am., 77, pp. 1688-1703.

Dermengian, J. M., J. R. Murphy and B. W. Barker (1985), "A Preliminary Analysis of Seismic Variability at the Shagan River Nuclear Test Site," SSS-R-86-7580, December.

Herrin, E., E. P. Arnold, B. A. Bolt, G. E. Clawson, E. R. Engdahl, H. W. Freedman, D. W. Gordon, A. L. Hales, J. L. Lobdell, O. Nuttli, C. Romney, J. Taggart, and W. Tucker (1968), "1968 Seismological Tables for P Phases," Bull. Seism. Soc. Am., 58, pp. 1193-1241.

Lay, T. and J. L. Welc (1987), "Analysis of Near-Source Contributions to Early P-Wave Coda for Underground Explosions. I. Waveform Complexity," Bull. Seism. Soc. Am., 77, pp. 1017-1040.

Marshall, P. D., T. C. Bache, and R. C. Lilwall (1984), "Body Wave Magnitudes and Locations of Soviet Underground Explosions at the Semipalatinsk Test Site," AWRE Report No. O-16/84, HMSO London.

APPENDIX A

Station-Corrected m_b Residuals as a Function of Shagan River Event Location For Selected GDSN Stations

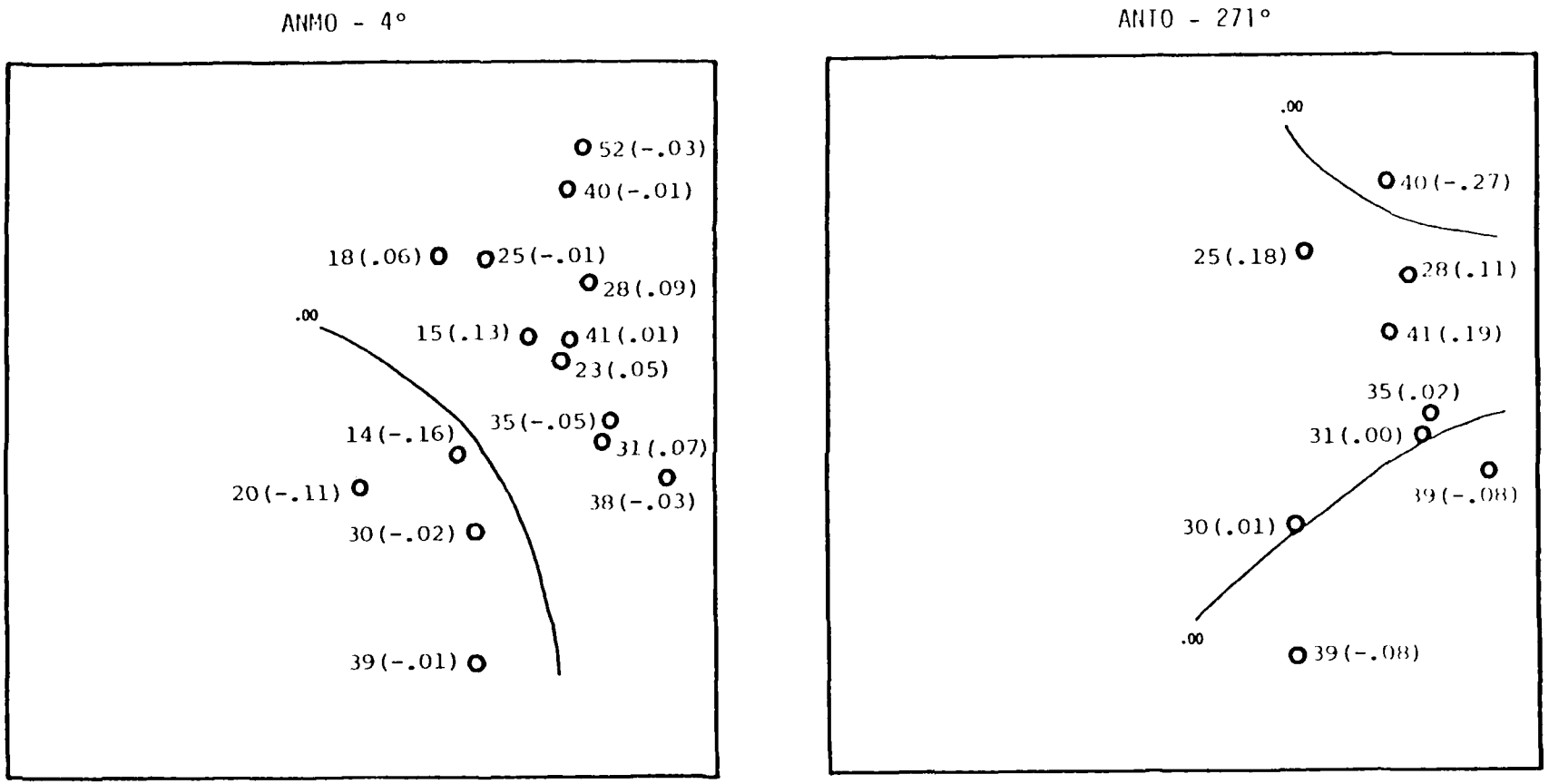

Figure A-1. Stations ANMO (left) and ANTO (right) at the denoted recording azimuths.

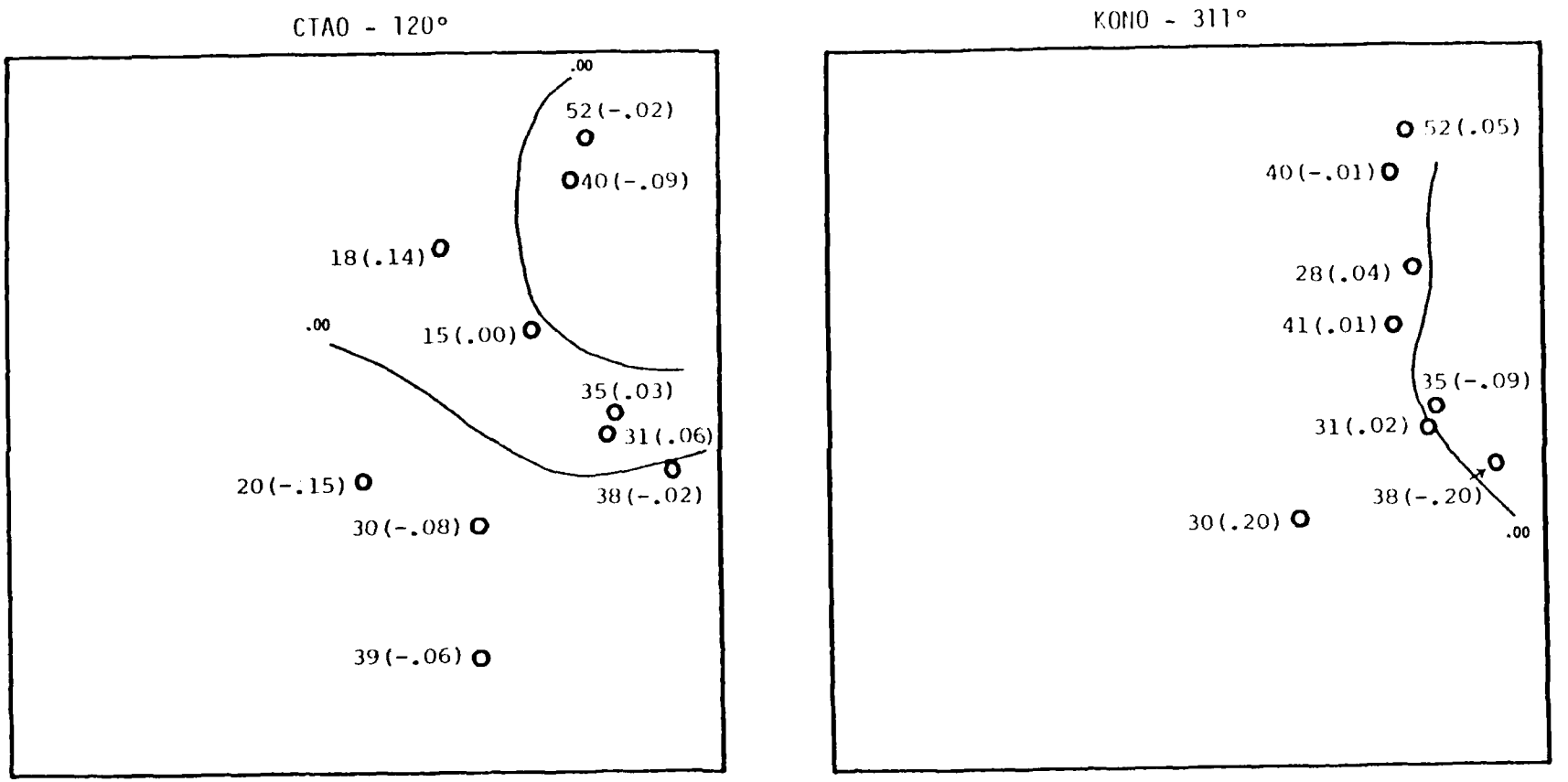

Figure A-2. Stations CTAO (left) and KONO (right) at the denoted recording azimuths.

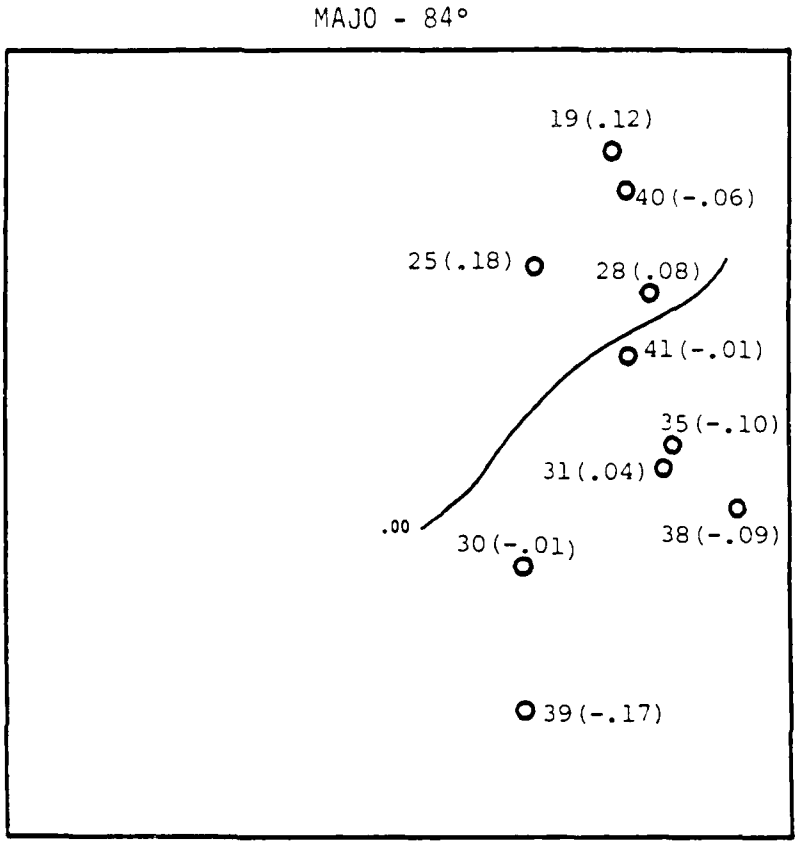

Figure A-3. Station MAJO at the denoted recording azimuth.

APPENDIX B

Teleseismic Short-Period P Waveforms Recorded at Selected GDSN Stations From Shagan River Explosions, in Order of Station m_b Residual

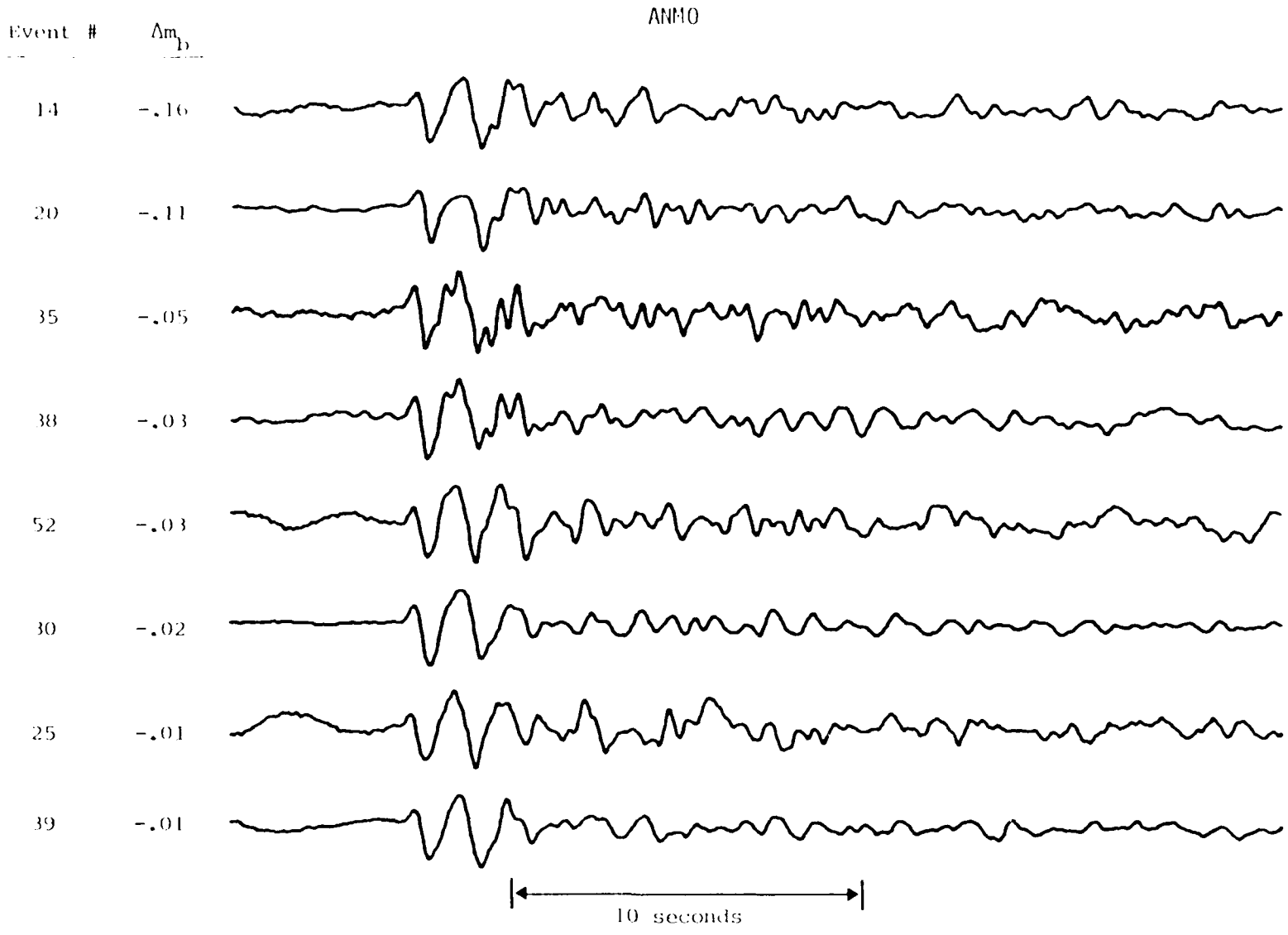

Figure B-1. Station ANMO.

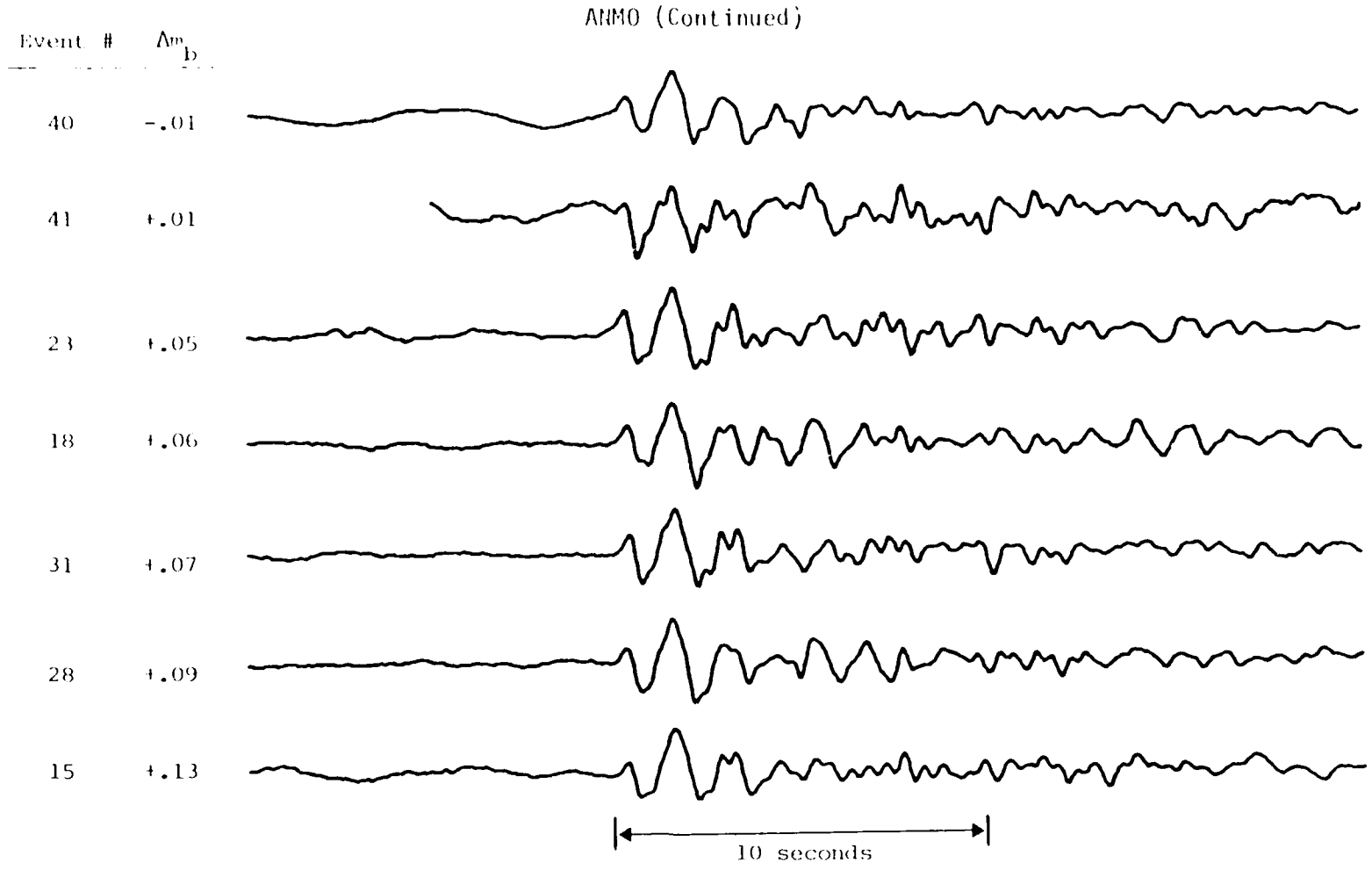

Figure B-1. Station ANMO (Continued).

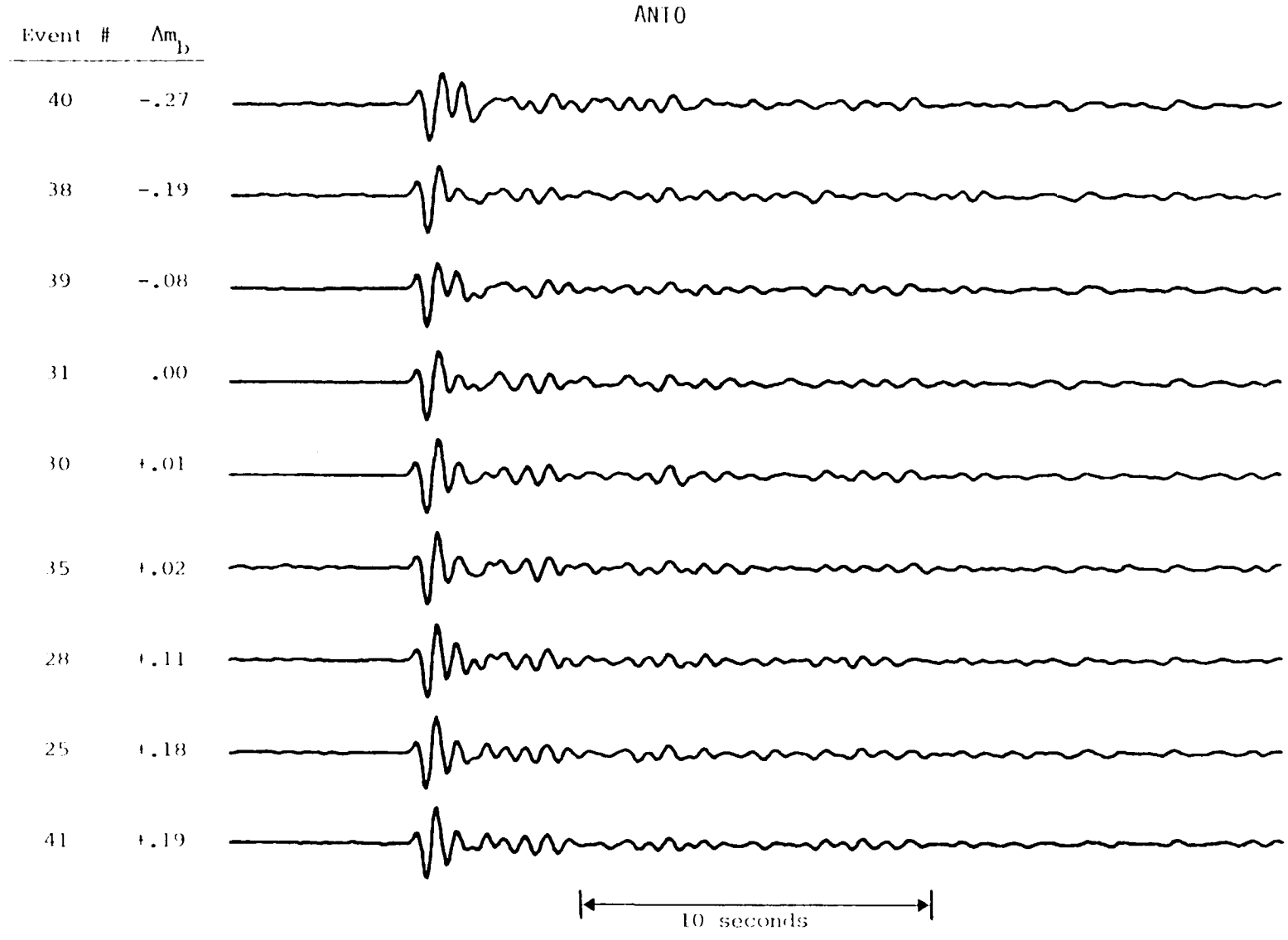

Figure B-2. Station ANTO.

CTAO

Event #	Δm_b
20	-.15
40	-.09
30	-.08
39	-.06
38	-.02
52	-.02
35	+.03
31	+.06
18	+.14

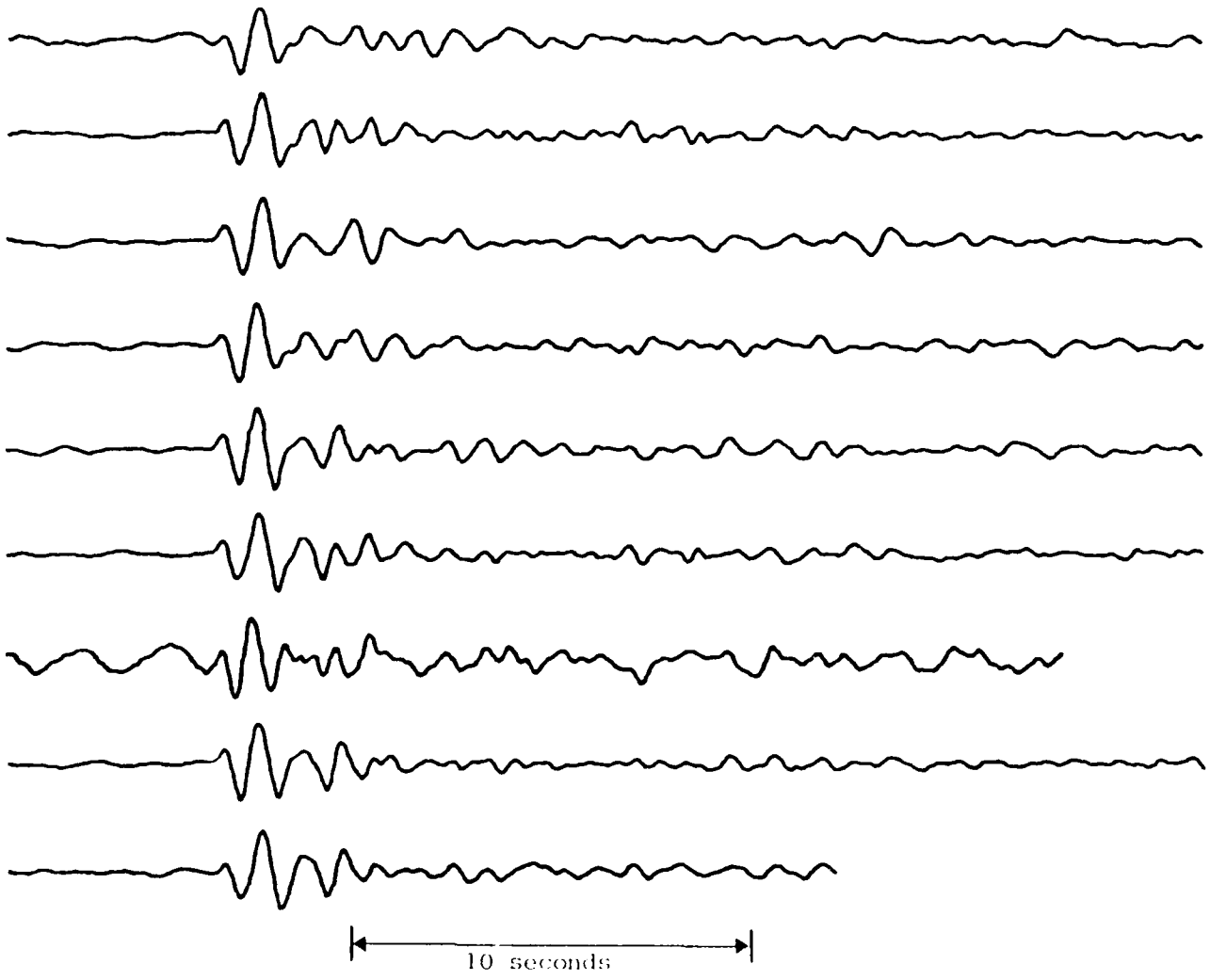

Figure B-3. Station CTAO.

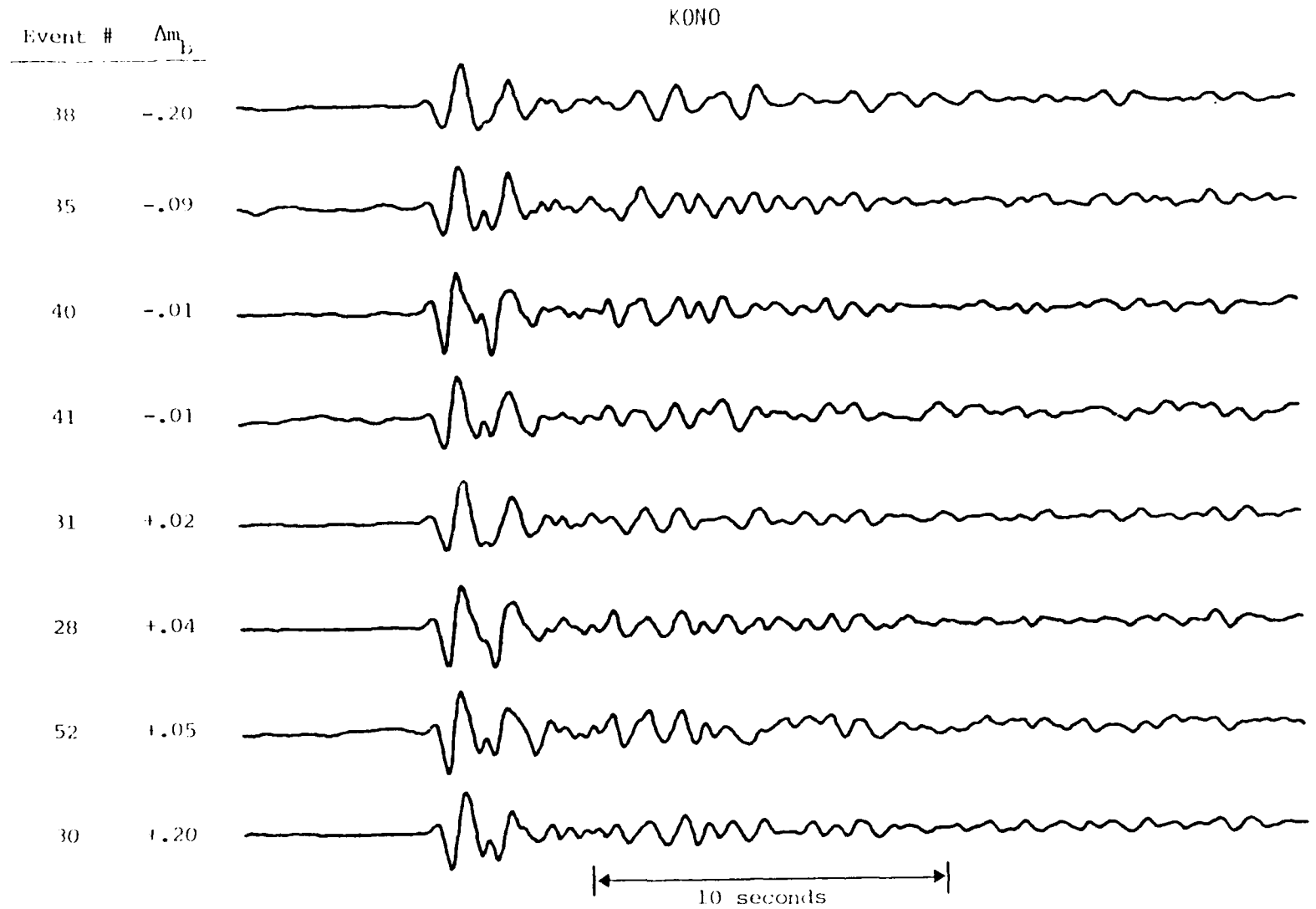

Figure B-4. Station KONO.

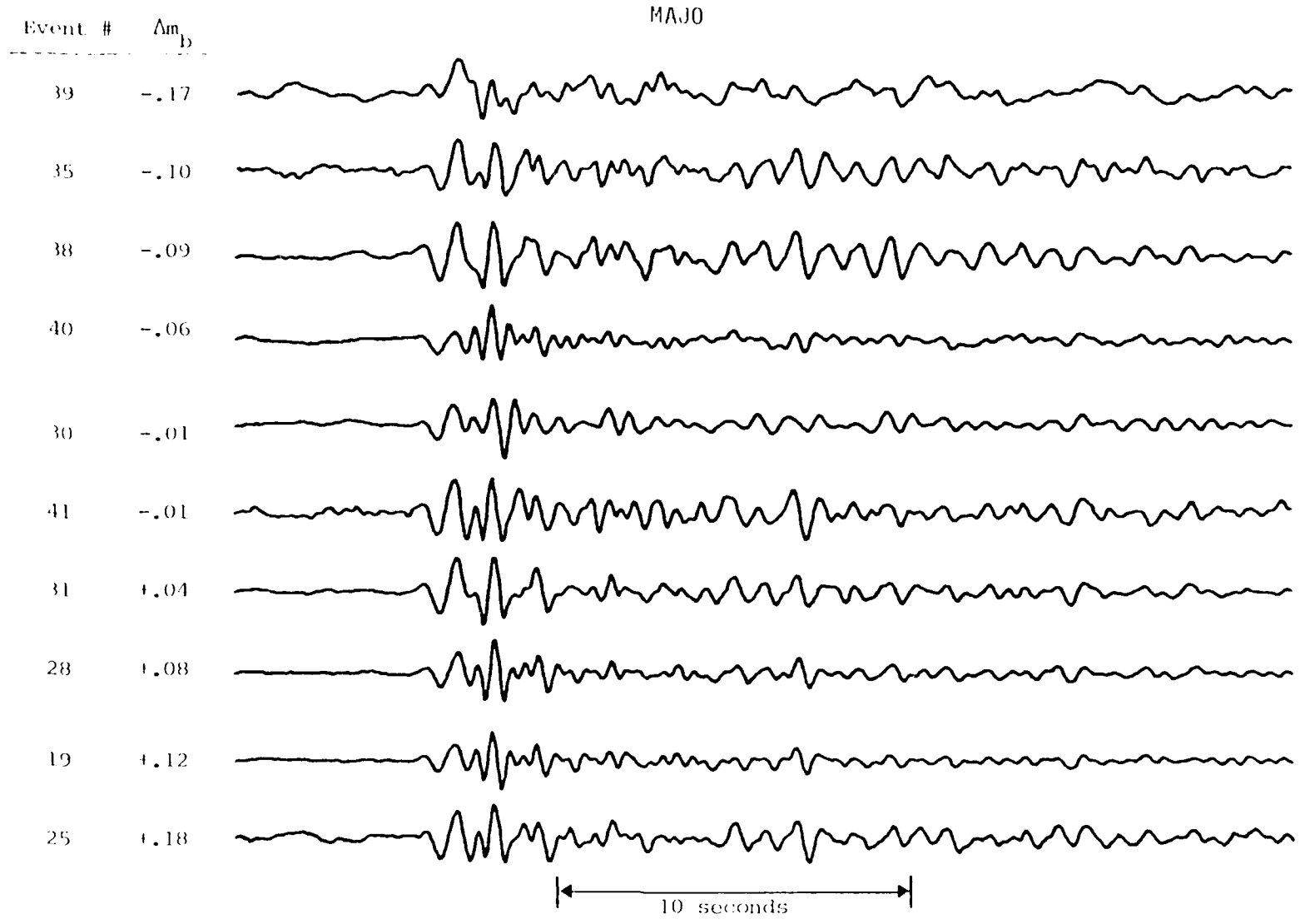

Figure B-5. Station MAJO.